

Optimization of Charge Collection and Radiation Hardness of Edgeless Silicon Pixel Sensors for Photon Science and HEP Applications

Jiaguo Zhang¹, Damaris Tartarotti Maimone², David Pennicard¹,
Milija Sarajlic¹, and Heinz Graafsma¹

¹*Deutsches Elektronen-Synchrotron (DESY), Germany*

²*Universidade Estadual de Campinas, Brasil*

Outline

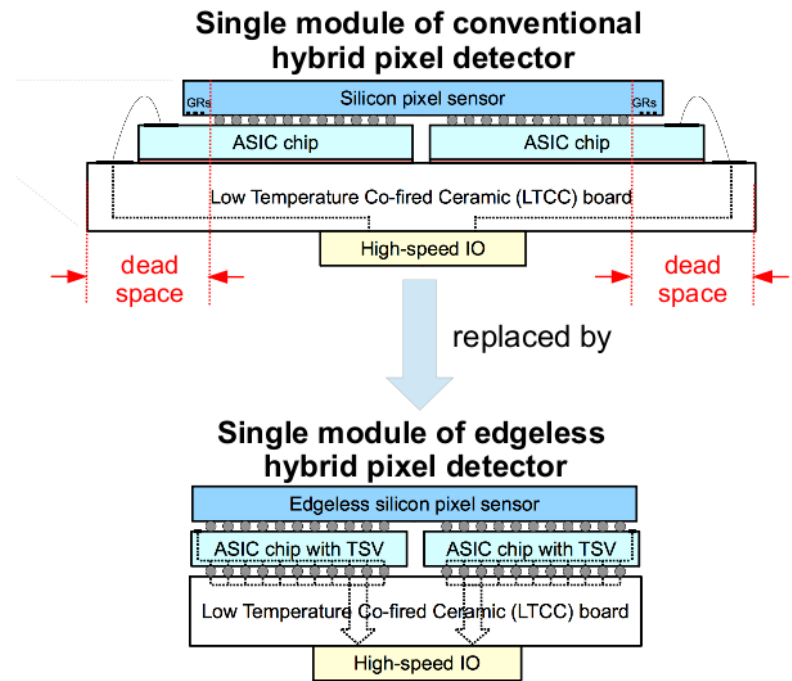
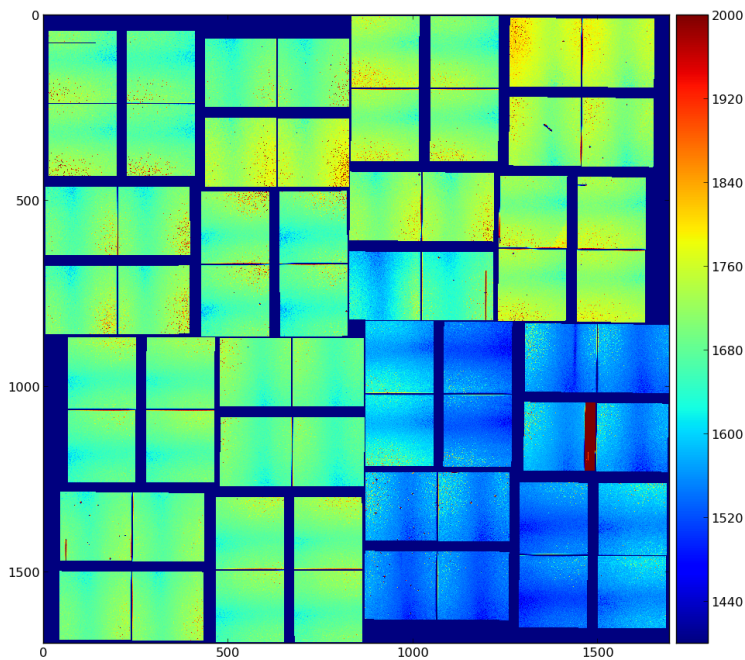
- Motivation
- Requirements and challenges of edgeless sensors
- Simulation of active volume and breakdown
- Modeling of charge-collection behavior
- Summary



Motivation of edgeless detectors in photon science

➤ Drawback of conventional large-area tiled hybrid pixel detectors

- information missing within dead space → problems in image reconstruction



➤ Goal: Development of edgeless hybrid silicon pixel detectors using

- [edgeless sensor](#) + [ASIC chips with TSV](#) + [chip-to-board integration through BGA](#)

Requirements and challenges of edgeless sensors

> Requirements of edgeless sensor for photon science application:

- Good quantum efficiency
- Full active sensor volume (no dead region)
- Small last pixel-to-edge distance (edge space)
- Low leakage current
- High breakdown voltage
- Radiation tolerant to ionizing radiation (surface damage)
- Consistent response to photons with different energies

Main challenges

> Procedures to optimize an edgeless sensor:

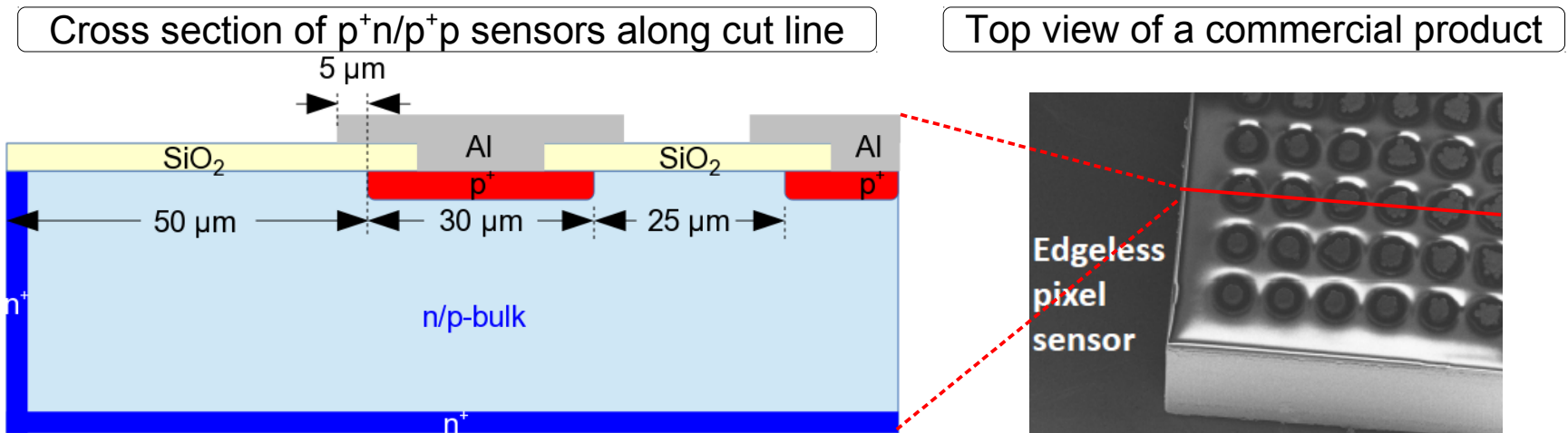
- TCAD simulations for edgeless sensors from available commercial designs
→ guideline for the sensor optimization with respect to technology choice
- Modeling charge-collection behavior of edgeless sensors
→ guideline for the choice of sensor thickness and last pixel-to-edge distance



Simulation of commercial edgeless sensors

➤ Layouts and cross sections of commercial edgeless sensors

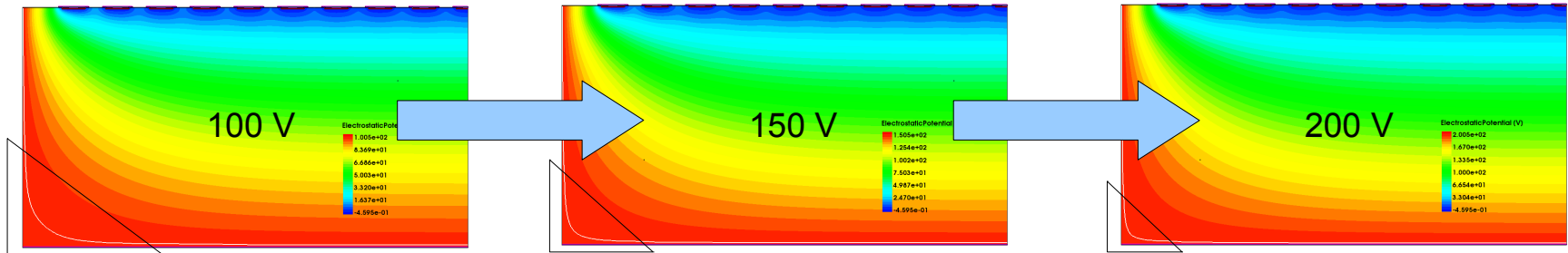
- 6 different layouts: p^+n , p^+p , n^+p and n^+n with p-spray, n^+p and n^+n with p-stop
- Si-thickness: 150 μm , 300 μm & 500 μm (only results for 300 μm to be shown)
- Last pixel-to-edge distance: 50 μm
- Junction depth of 1.2 μm and oxide thickness of 700 nm



➤ Radiation-damage parameters (N_{ox} & S_0) from measurements input

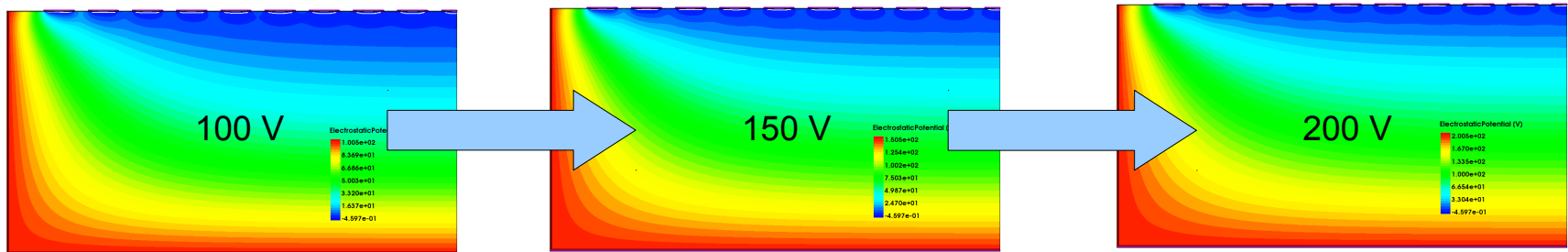
Simulation of sensor active/depletion volume

> Active volume of p⁺n and n⁺p (p-stop/p-spray) sensors



- Inactive volume shrinks with voltage (at least 100 V above V_{dep} needed?)
- Higher doping, thicker Si → larger additional voltage needed

> Active volume of n⁺n (p-stop/p-spray) and p⁺p sensors

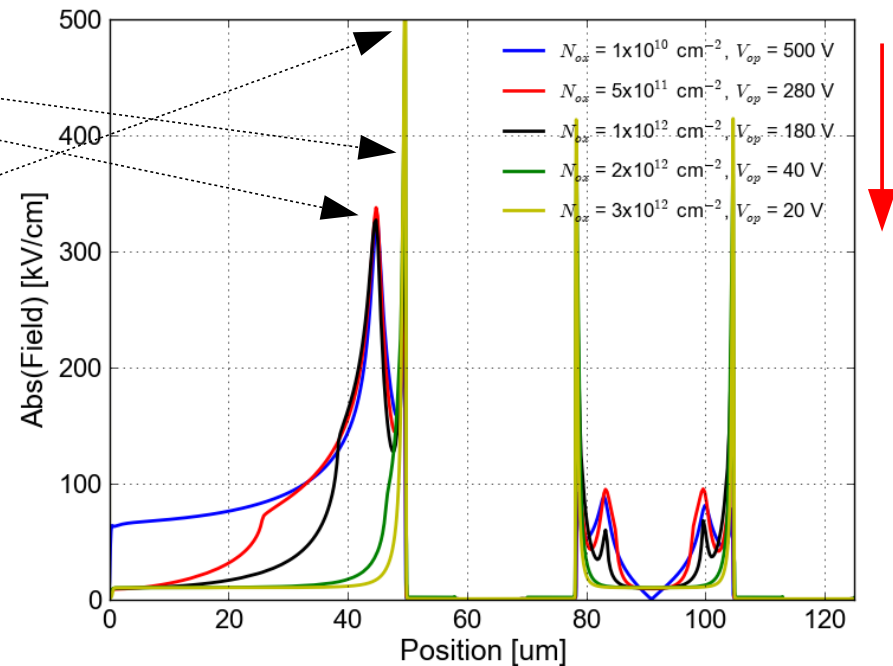
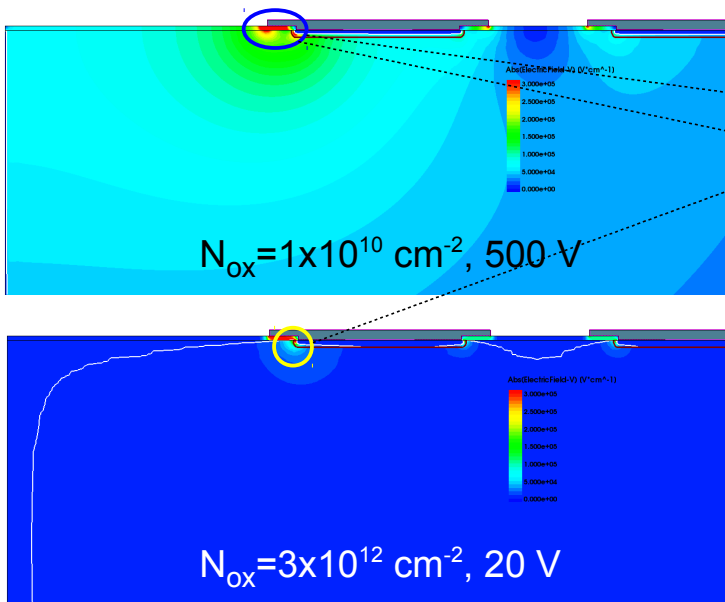


- Sensor depletion starting from edge and backside → no inactive region
- No/Small additional voltage above V_{dep} needed (typically 10-15 V)

Breakdown simulation of p⁺n (p⁺p) sensor

➤ High field region:

- $N_{ox} \leq 1 \times 10^{12} \text{ cm}^{-2}$, high field below metal overhang and at junction of 1st pixel
- $N_{ox} > 1 \times 10^{12} \text{ cm}^{-2}$, high field at implant junction of 1st pixel

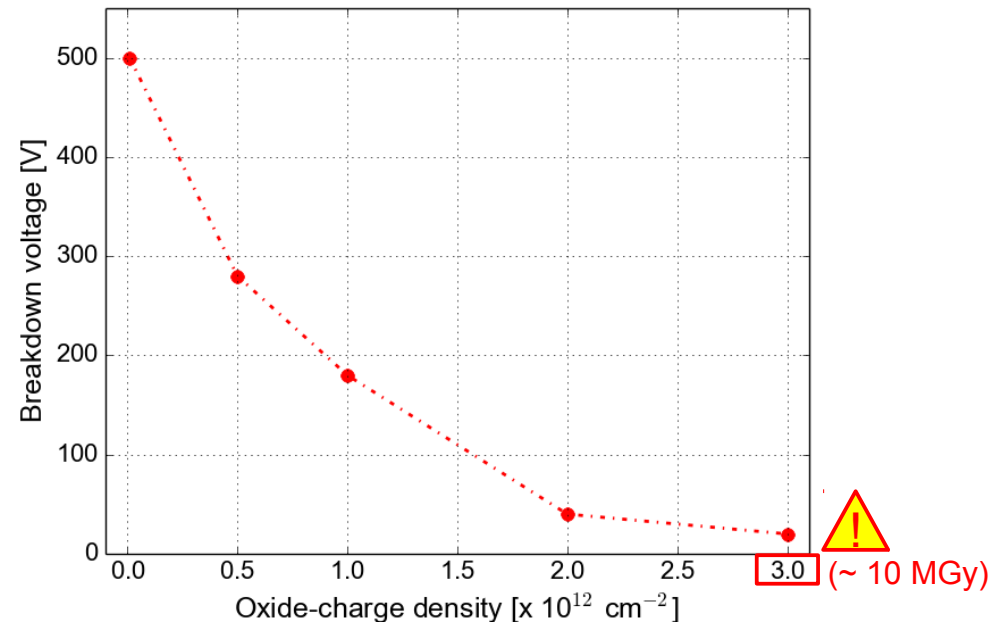
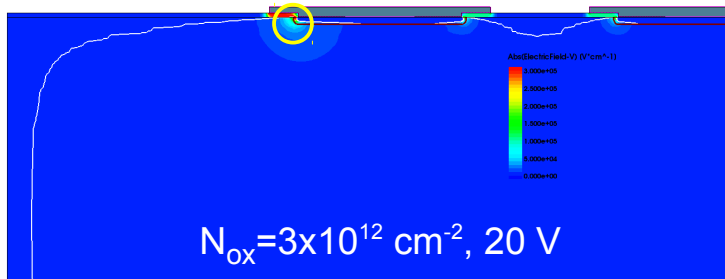
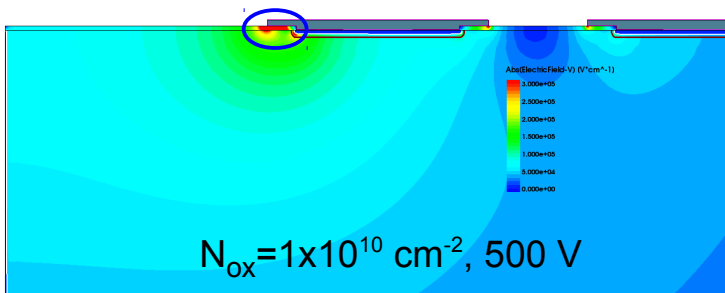


- 1st pixel behaves like CCR of a conventional sensor → breakdown first
- Breakdown voltage drops gradually with increasing oxide charges

Breakdown simulation of p⁺n (p⁺p) sensor

➤ High field region:

- $N_{ox} \leq 1 \times 10^{12} \text{ cm}^{-2}$, high field below metal overhang and at junction of 1st pixel
- $N_{ox} > 1 \times 10^{12} \text{ cm}^{-2}$, high field at implant junction of 1st pixel

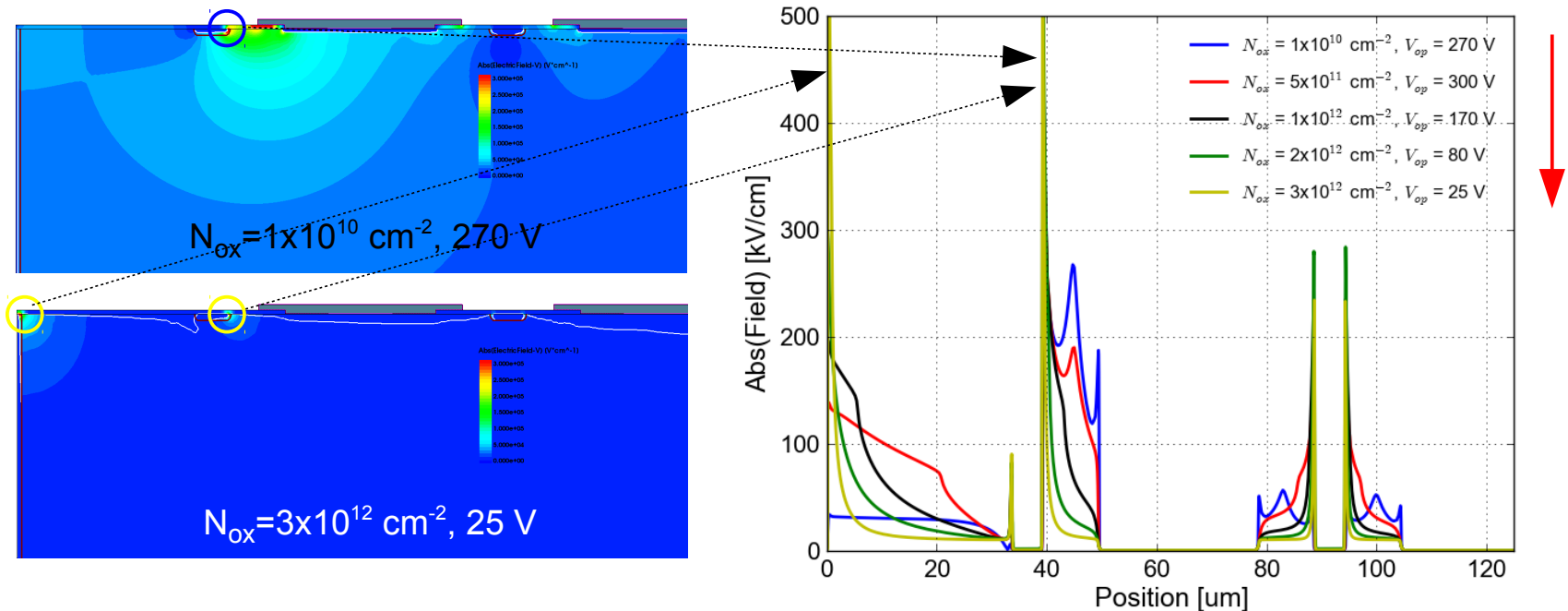


- 1st pixel behaves like CCR of a conventional sensor → breakdown first
- Breakdown voltage drops gradually with increasing oxide charges

Breakdown simulation of n⁺n (n⁺p) sensors with p-stop

➤ High field region:

- $N_{ox} \leq 1 \times 10^{12} \text{ cm}^{-2}$, high field at implant junction of p-stop
- $N_{ox} > 1 \times 10^{12} \text{ cm}^{-2}$, high field at implant junctions of p-stop and sensor edge

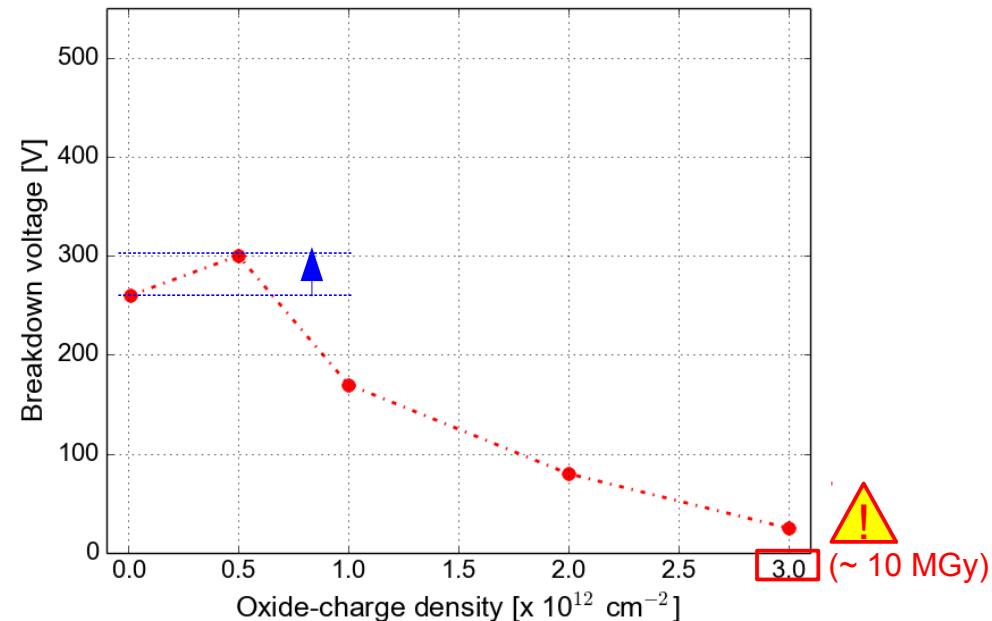
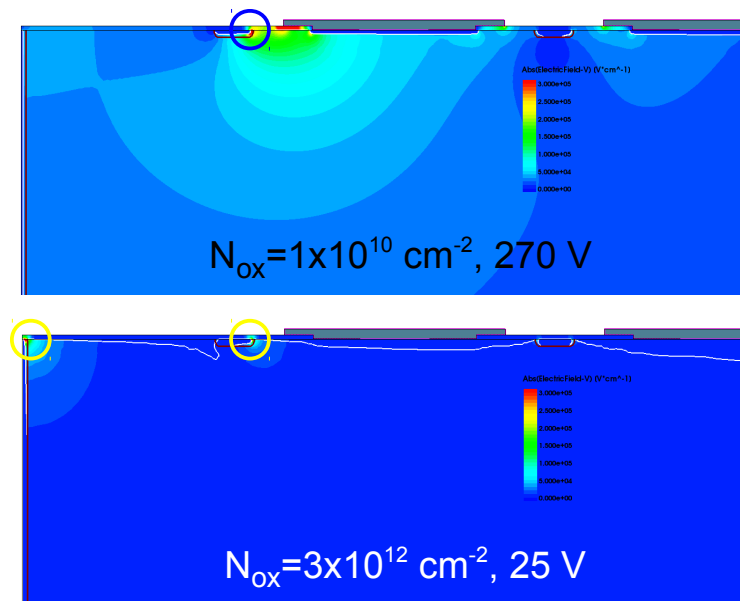


- High field at sensor edge ← direct exposure to oxide charges
- Breakdown voltage drops to 25 V at high oxide charges!

Breakdown simulation of n⁺n (n⁺p) sensors with p-stop

➤ High field region:

- $N_{ox} \leq 1 \times 10^{12} \text{ cm}^{-2}$, high field at implant junction of p-stop
- $N_{ox} > 1 \times 10^{12} \text{ cm}^{-2}$, high field at implant junctions of p-stop and sensor edge

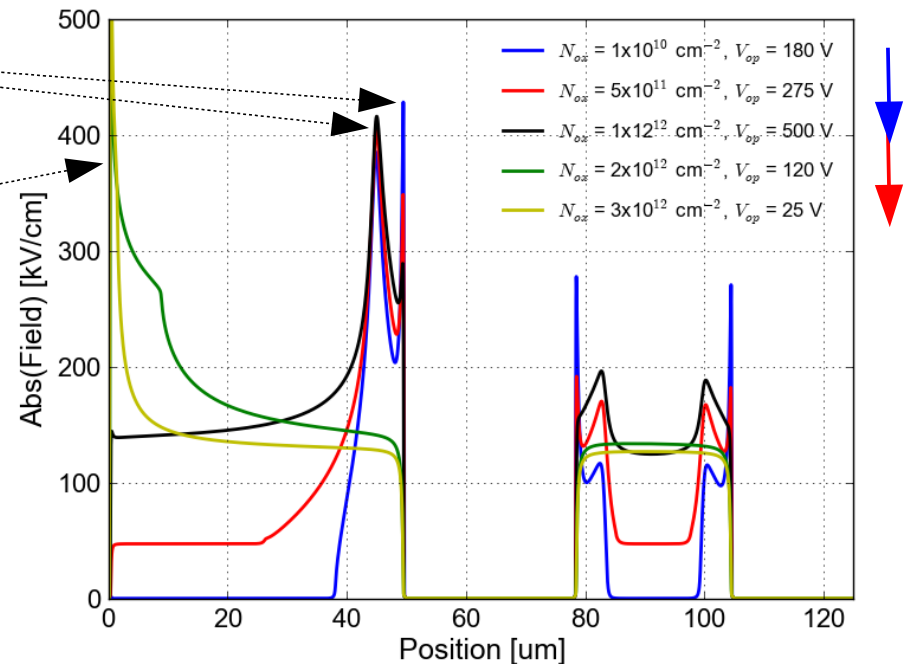
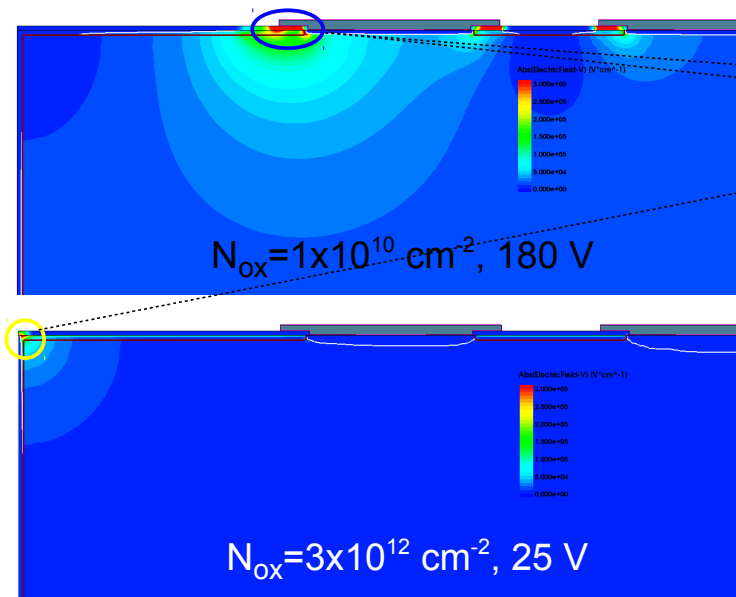


- High field at sensor edge ← direct exposure to oxide charges
- Breakdown voltage drops to 25 V at high oxide charges!

Breakdown simulation of n⁺n (n⁺p) sensors with p-spray

➤ High field region:

- $N_{ox} \leq 1 \times 10^{12} \text{ cm}^{-2}$, high field at pixel-implant/p-spray interface and below metal
- $N_{ox} > 1 \times 10^{12} \text{ cm}^{-2}$, high field at sensor edge

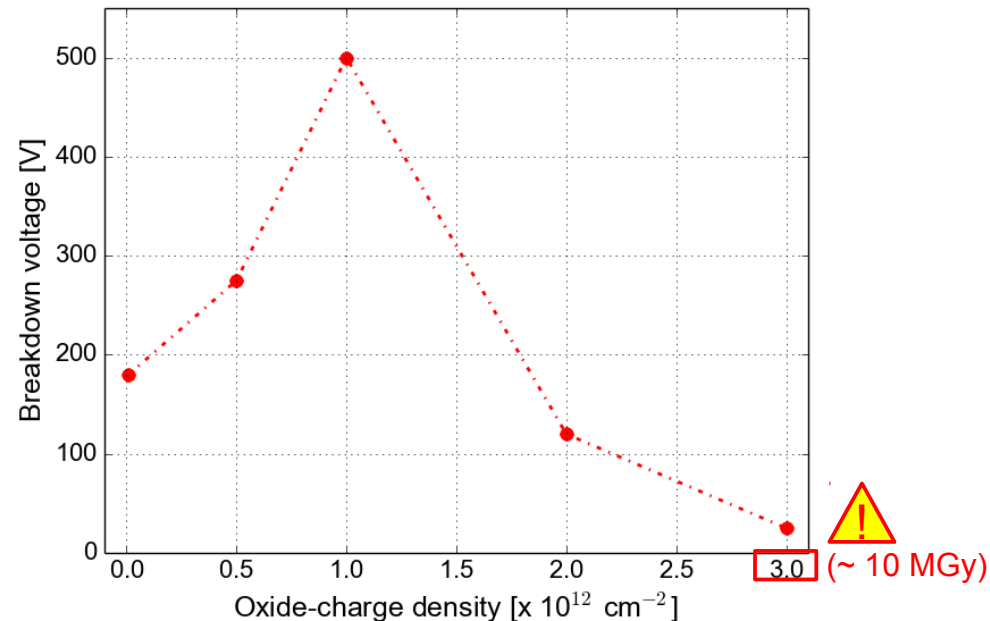
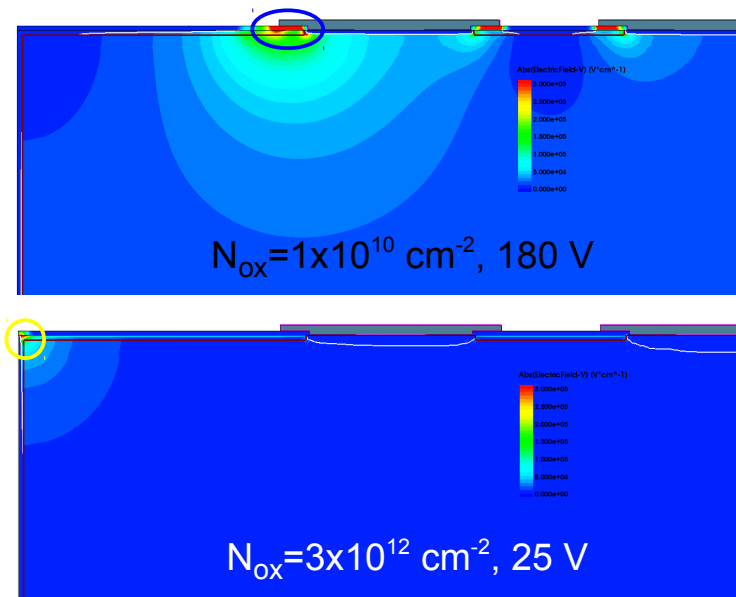


- High field at sensor edge → improved by increasing p-spray dose
- Breakdown improves with N_{ox} , but decreases when $N_{ox} > N_{p-spray}$

Breakdown simulation of n⁺n (n⁺p) sensors with p-spray

➤ High field region:

- $N_{ox} \leq 1 \times 10^{12} \text{ cm}^{-2}$, high field at pixel-implant/p-spray interface and below metal
- $N_{ox} > 1 \times 10^{12} \text{ cm}^{-2}$, high field at sensor edge



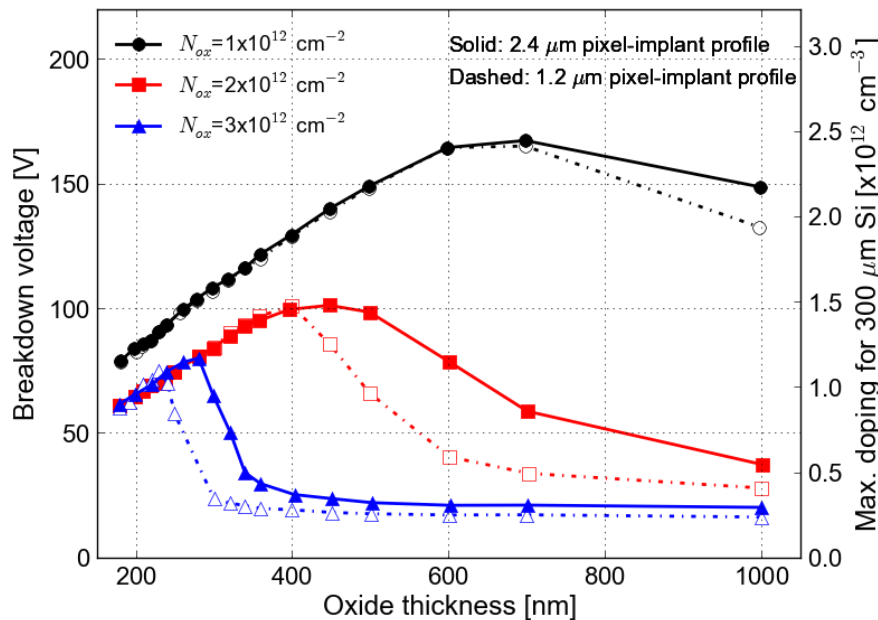
➤ High field at sensor edge → improved by increasing p-spray dose

➤ Breakdown improves with N_{ox} , but decreases when $N_{ox} > N_{p-spray}$

How to improve the radiation hardness of edgeless sensors

➤ Lessons learnt from AGIPD p⁺n sensors:

- Improved breakdown voltage with optimized technological parameters
- 75 V per guard ring → guard ring needed for high operation voltage



Min. requirement for sensor operation:

$$V_{dep} = \frac{q_0 T_{si}^2 N_d}{2\epsilon_0 \epsilon_{si}} - V_{bi} < V_{bd}$$

→ max. doping N_d

e.g. for 700 nm SiO₂, $N_d < 3 \times 10^{11} \text{ cm}^{-3}$
is required for full depletion of a
300 μm thick Si.

➤ Indication for edgeless sensors: careful selection of tech. parameters

- [Junction depth](#) + [oxide thickness](#) + [doping concentration in Si](#)

➤ Similar optimization procedures for other polarities

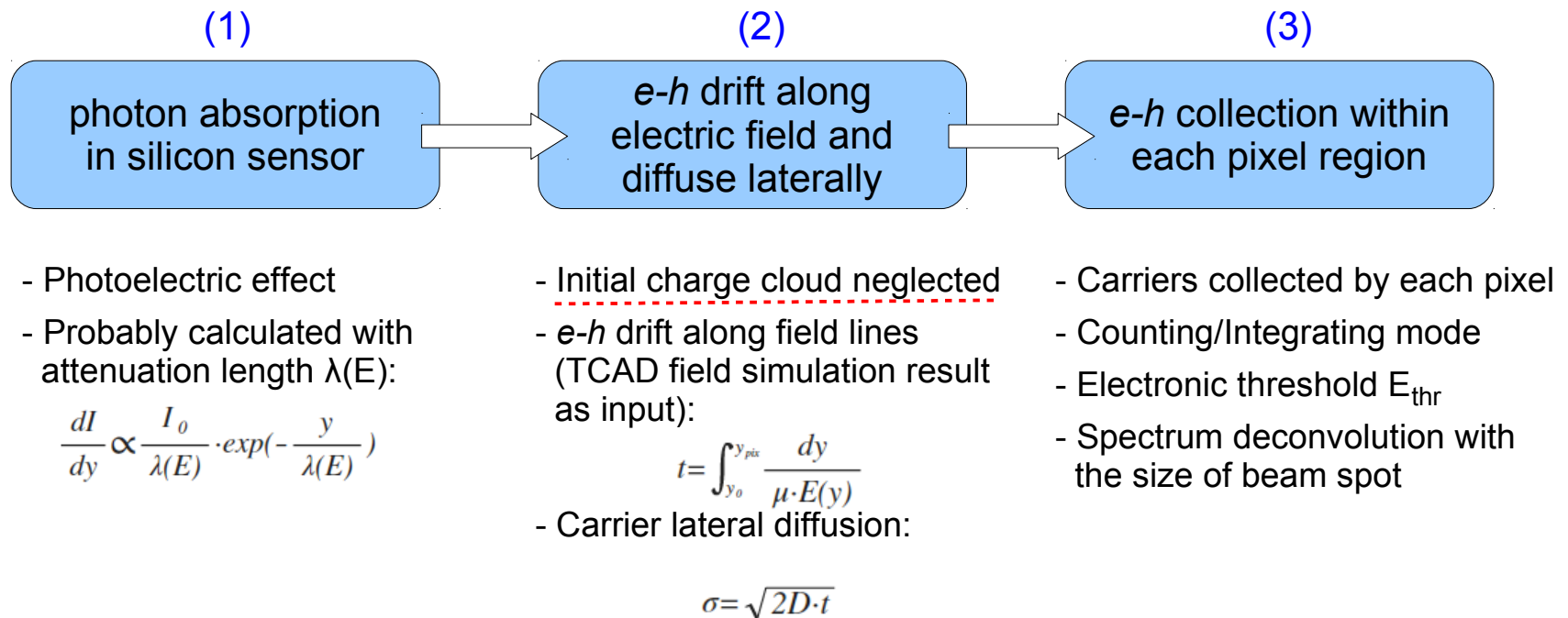


Charge-collection behavior: Model development

> Motivation of modeling charge collection of edgeless sensors:

- Understand measurement results with developed model
- Predict charge-collection behavior for sensors with different thicknesses
- Optimize sensor layout with best charge-collection behavior

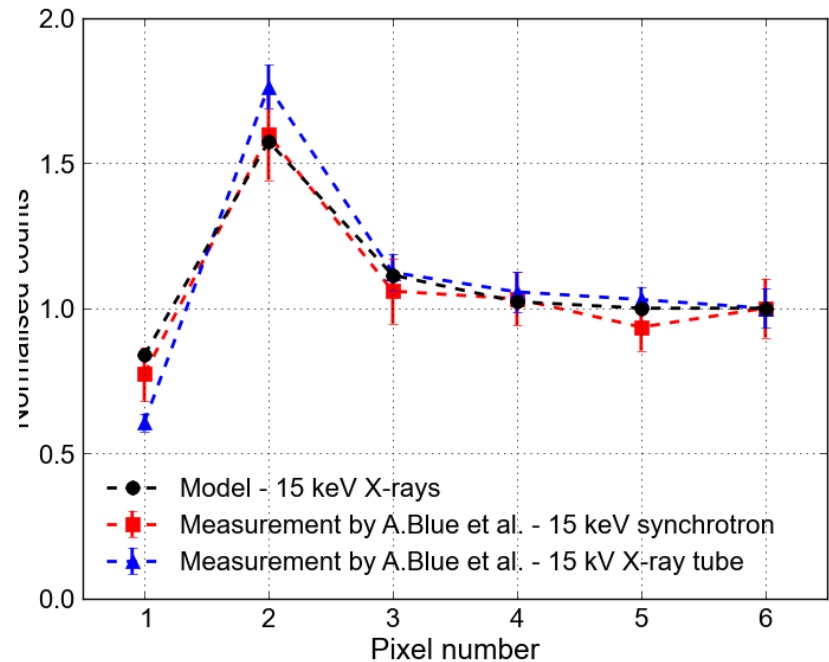
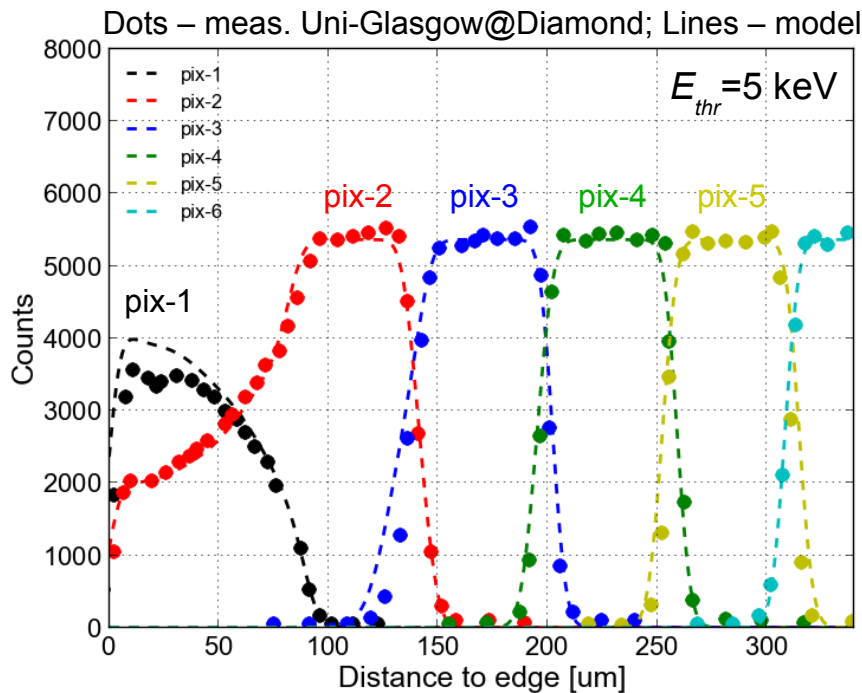
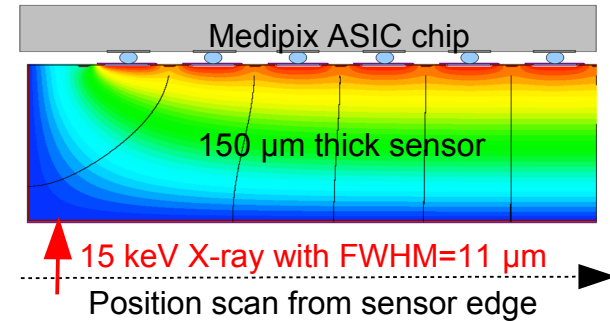
> The physics model for $E_{x\text{-ray}} < 20 \text{ keV}$ (can/to be extended):



Charge-collection behavior: Comparison to measurements

➤ From model calculation to measurement result:

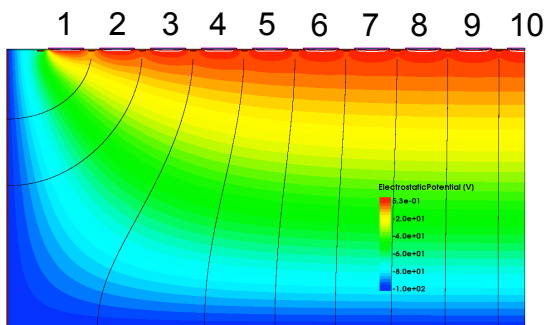
- 15 keV X-rays with FWHM = 11 μm
- 150 μm thick sensor
- X-ray backside scan from sensor edge



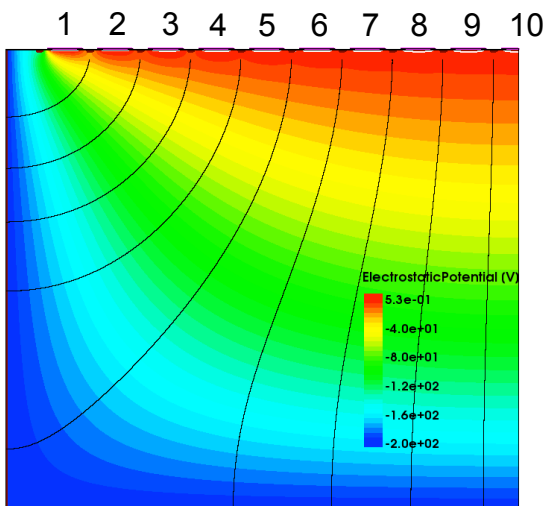
➤ Measurement results explained by developed model!

Charge-collection behavior: Prediction

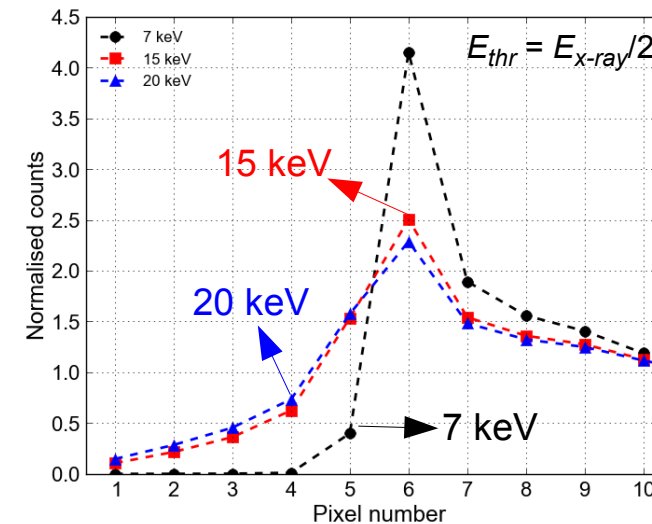
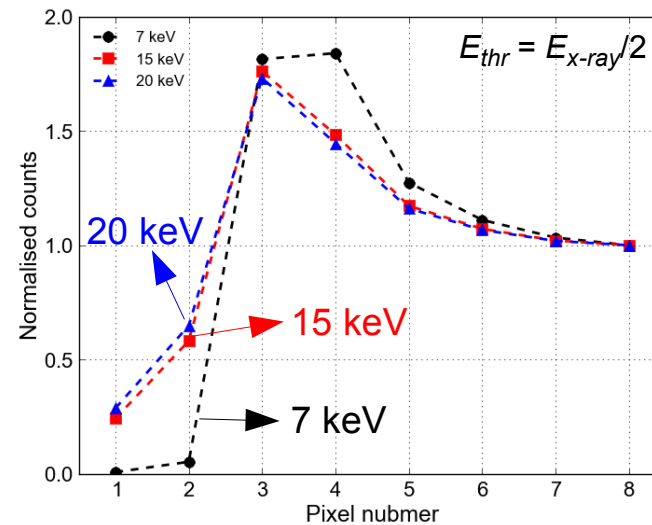
➤ Charge-collection behavior of edge pixels for thick Si sensors:



300 μm thick sensor
(volume full depleted)

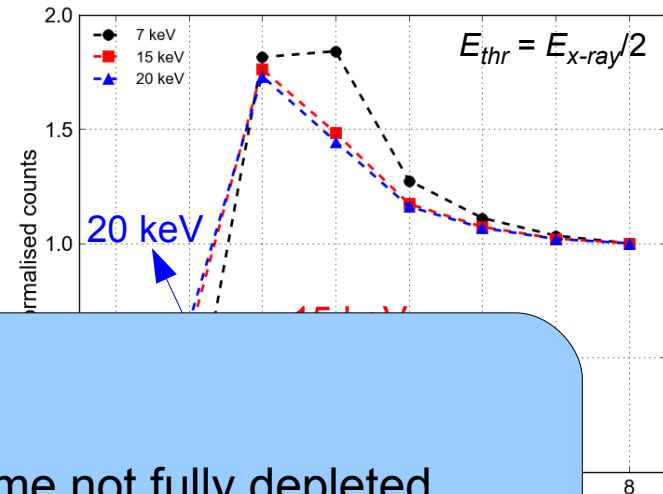
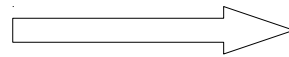
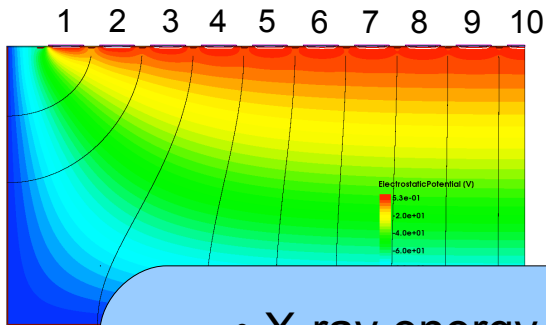


500 μm thick sensor
(volume full depleted)

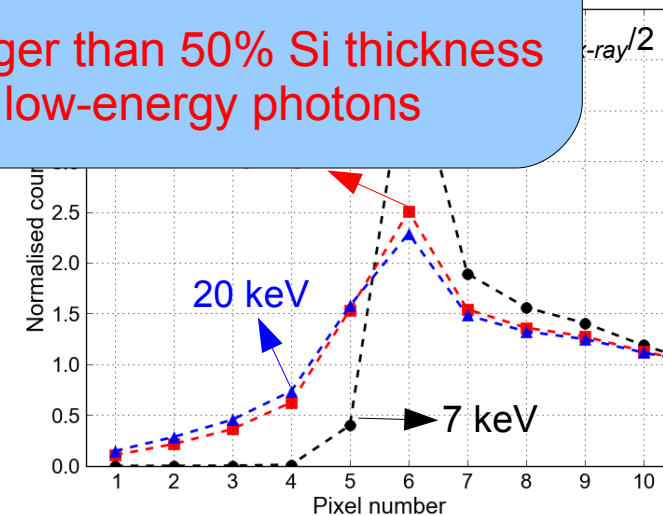
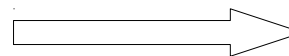
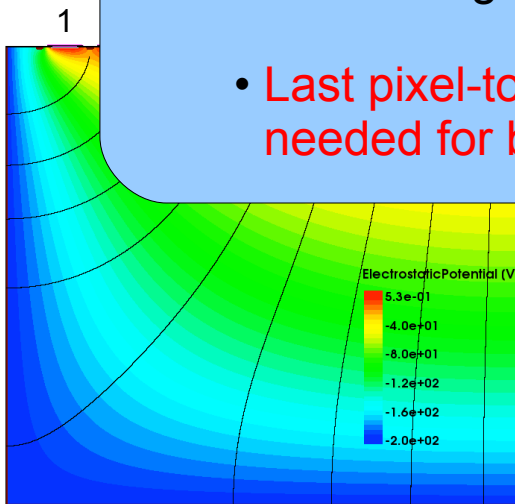


Charge-collection behavior: Prediction

➤ Charge-collection behavior of edge pixels for thick Si sensors:



- X-ray energy dependent
- Sensor thickness dependent
- Bias voltage dependent if volume not fully depleted
- Last pixel-to-edge distance larger than 50% Si thickness needed for better sensitivity to low-energy photons



500 μm thick sensor
(volume full depleted)

Summary and conclusion

- Current understanding on edgeless sensors based on TCAD simulation and model calculation
- TCAD simulations with measurement parameters implemented used for the understanding of
 - Sensor active volume
 - Breakdown
 - Radiation tolerance
- To improve radiation hardness, careful selection of technological parameters and doping concentration
- Model developed for the understanding of charge-collection behavior of edgeless sensors:
 - Measurement results explained by developed model
 - Charge-collection behaviors predicted for thicker Si
- To ensure sensitivity of edge pixels to low energy photons, last pixel-to-edge distance should be $> 50\%$ Si-thickness



Acknowledgements

LAMBDA

David Pennicard, Sergej Smoljanin,
Sabine Lange, Helmut Hirsemann,
Bernd Struth, Fabian Westermeier,
Andre Rothkirch, Yuelong Yu, Heinz
Graafsma

– **DESY, Hamburg**

Milan Zuvic, Marie-Odile Lampert
– **Canberra France, Lingsheim**

Thomas Fritsch, Mario Rothermund
– **Fraunhofer IZM, Berlin**

Michael Epple
– **TU Munich**



Aschkan Allahgholi², Julian Becker², Laura Bianco²,
Roberto Dinapoli¹, Peter Goettlicher², Heinz
Graafsma^{2,5}, Dominic Greiffenberg¹, Helmut
Hirsemann², Stefanie Jack², Robert Klanner³,
Alexander Klyuev², Hans Krueger⁴, Sabine Lange²,
Alessandro Marras², Davide Mezza¹, Aldo
Mozzanica¹, Seungyu Rah², Qingqing Xia², Bernd
Schmitt¹, Joern Schwandt³, Igor Sheviakov², Xintian
Shi¹, Ulrich Trunk², Jiaguo Zhang², Manfred
Zimmer²

¹**Paul-Scherrer-Institut (PSI), SLS Detector Group,
Villigen, Switzerland**

²**DESY, Hamburg, Germany**

³**University of Hamburg, Hamburg, Germany**

⁴**University of Bonn, Bonn, Germany**

⁵**Mid Sweden University, Sundsvall, Sweden**



Matthias Bayer, Jonathan Correa, Heinz Graafsma,
Peter Göttlicher, Sabine Lange, Alessandro Marras,
Florian Pithan, Igor Sheviakov, Sergej Smoljanin,
Maximilian Tennert, Michele Viti, Qingqing Xia,
Manfred Zimmer

– **DESY, Hamburg**

Julien Marchal, Ulrik Pedersen, Nick Rees, Nicola
Tartoni, Jon Thompson

- **Diamond**

Giuseppe Cautero, Dario Giuressi, Ralf Menk, Luigi
Stebel, Hazem Yousef

- **Elettra**

Dipayan Das, Nicola Guerrini, Ben Marsh, Iain
Sedgwick, Renato Turchetta

- **RAL / STFC**

There are open positions for PostDocs and Master/PhD students!

http://photon-science.desy.de/research/technical_groups/detectors/index_eng.html



Thanks go to...

- Thanks for your attention!
- Thank Juha Kalliopuska of Advacam co. for providing technological parameters for simulation, and Dima Maneuski of Uni-Glasgow sharing the measurement data at Diamond beamline for comparison of results.

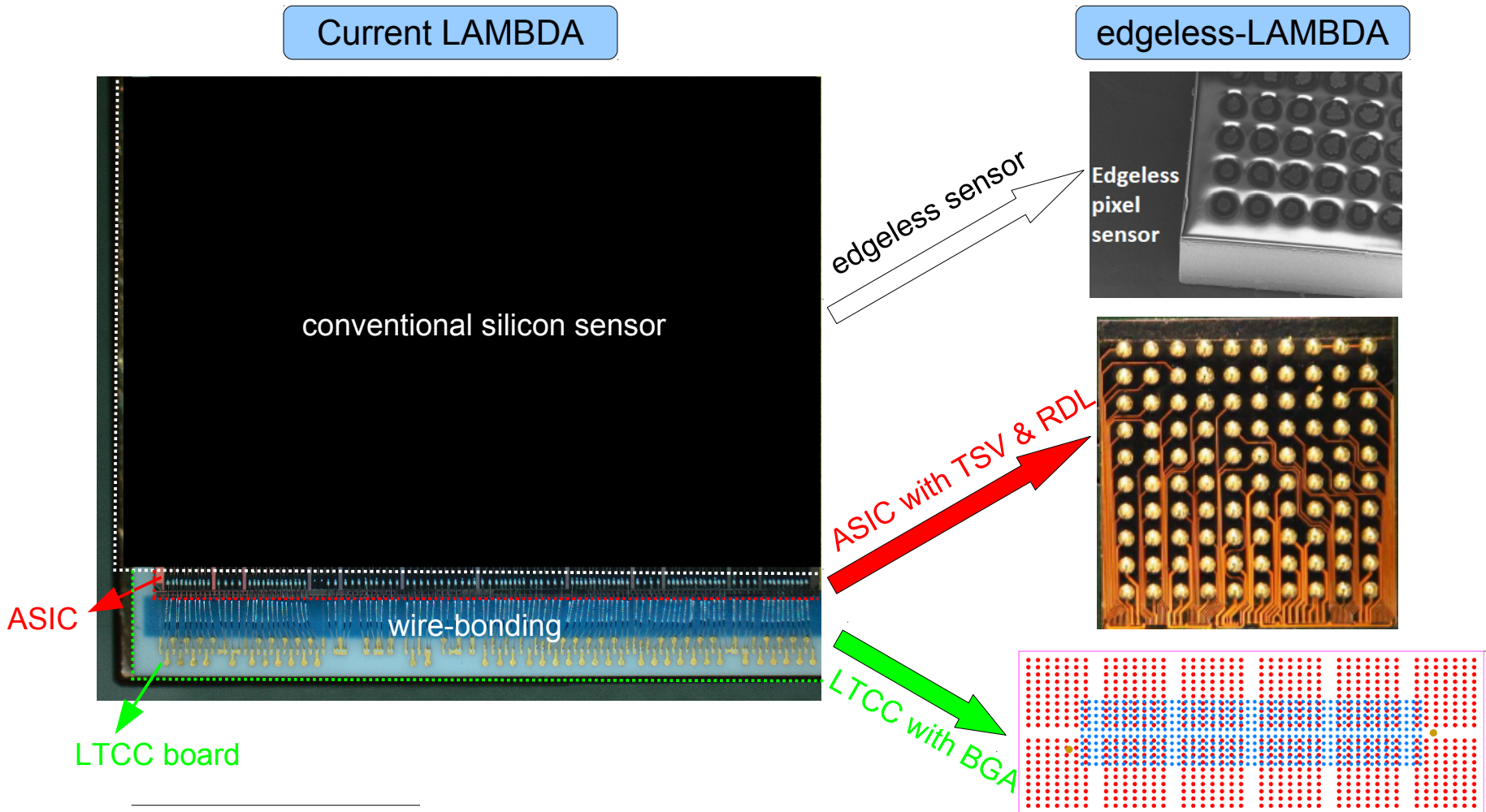


Backup slides



Development of edgeless detector @ DESY

> LAMBDA*-based edgeless detector as an example



*More information see the talk of D. Pennicard

Requirements and challenges of edgeless sensors

> Requirements of edgeless sensor for photon science application:

- Good quantum efficiency
- Full active sensor volume (no dead region)
- Small last pixel-to-edge distance (edge space)
- Low leakage current
- High breakdown voltage
- Radiation tolerant to ionizing radiation (surface damage)
- Consistent response to photons with different energies

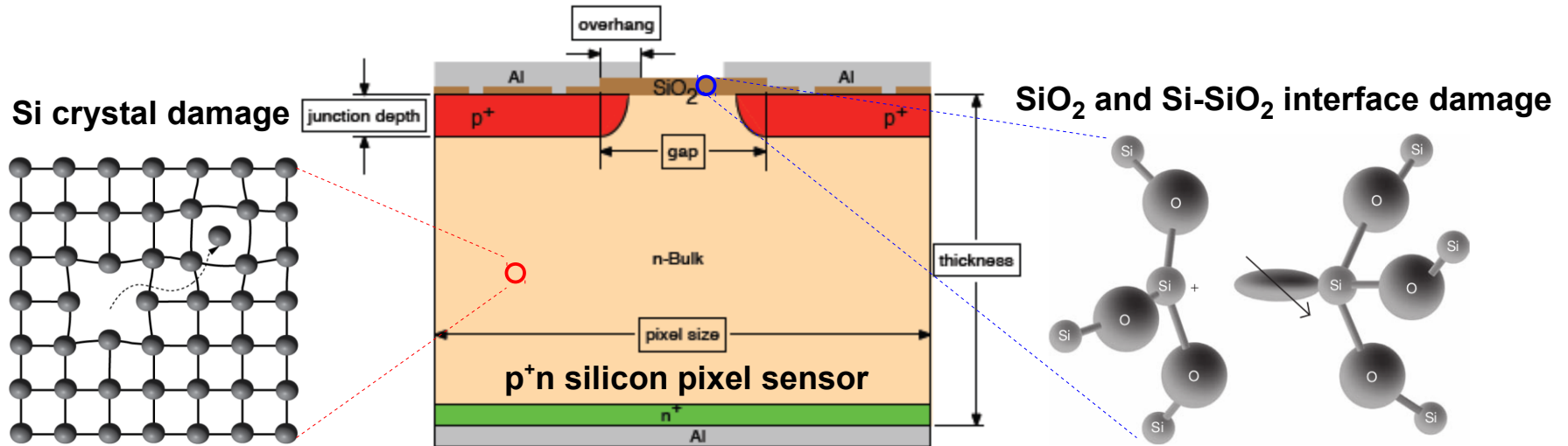
Main challenges

> Procedures to optimize an edgeless sensor:

- Understand electrical properties and radiation hardness of edgeless sensors from available commercial designs according to TCAD simulations
→ guideline for the sensor optimization with respect to technology choice
- Understand charge-collection behavior of edgeless sensors with different Si thicknesses by measurements and model calculation
→ guideline for the choice of sensor thickness and last pixel-to-edge distance



Introduction to radiation damage



> Bulk damage (Si crystal damage):

- Non Ionizing Energy Loss of incident particles (gamma-rays, electrons and hadrons) in silicon
- Clusters of defects/or and point defects (Vacancy + Interstitial)

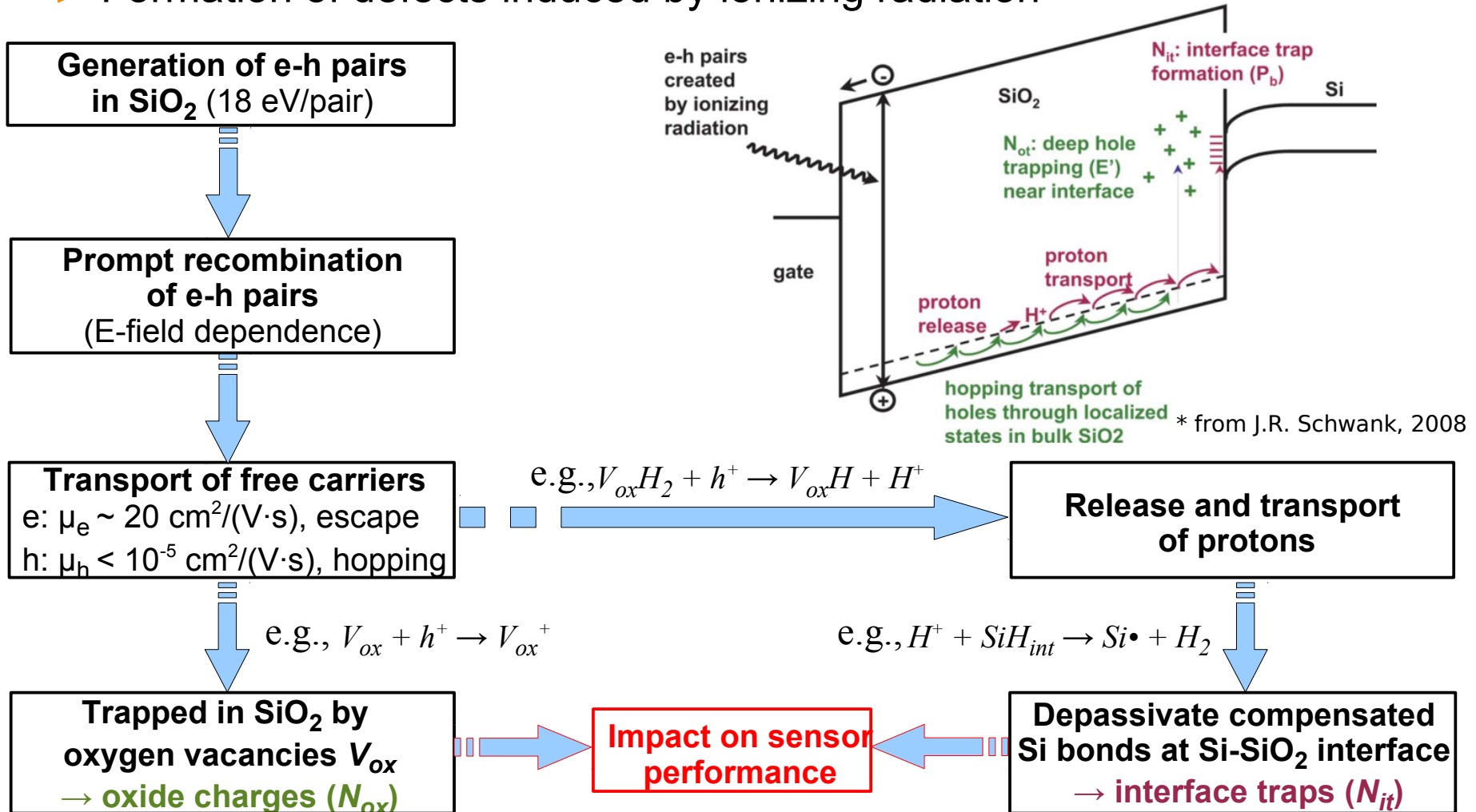
> Surface damage (SiO₂ and Si-SiO₂ interface damage):

- Ionizing Energy Loss of "charged" particles and X-rays in SiO₂
- Types of defects: Oxide charges, interface traps and etc.

Main concern in photon science & increased interest from HL-LHC

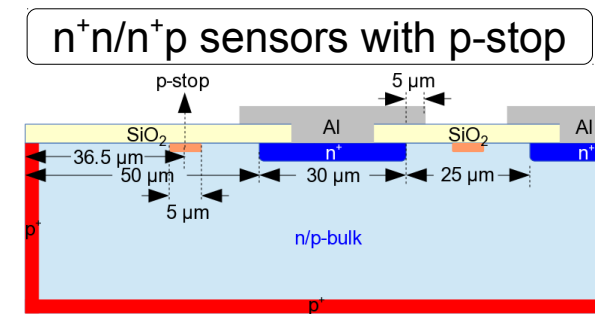
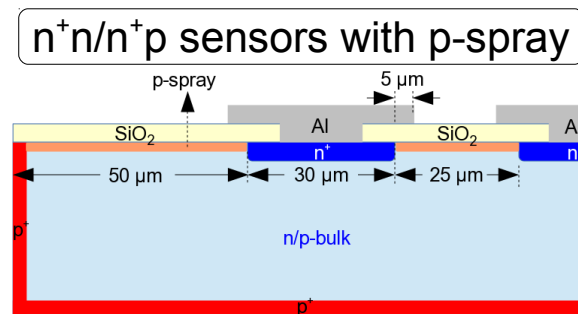
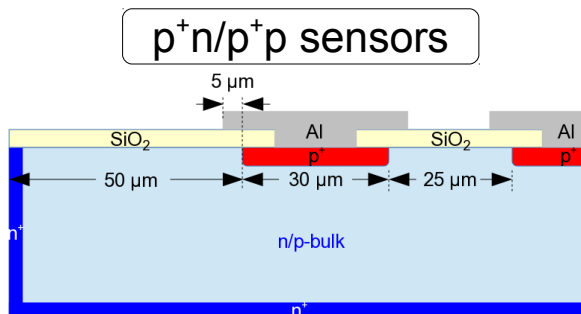
Mechanism of radiation-induced surface damage

> Formation of defects induced by ionizing radiation



Simulation of edgeless sensors: Layouts

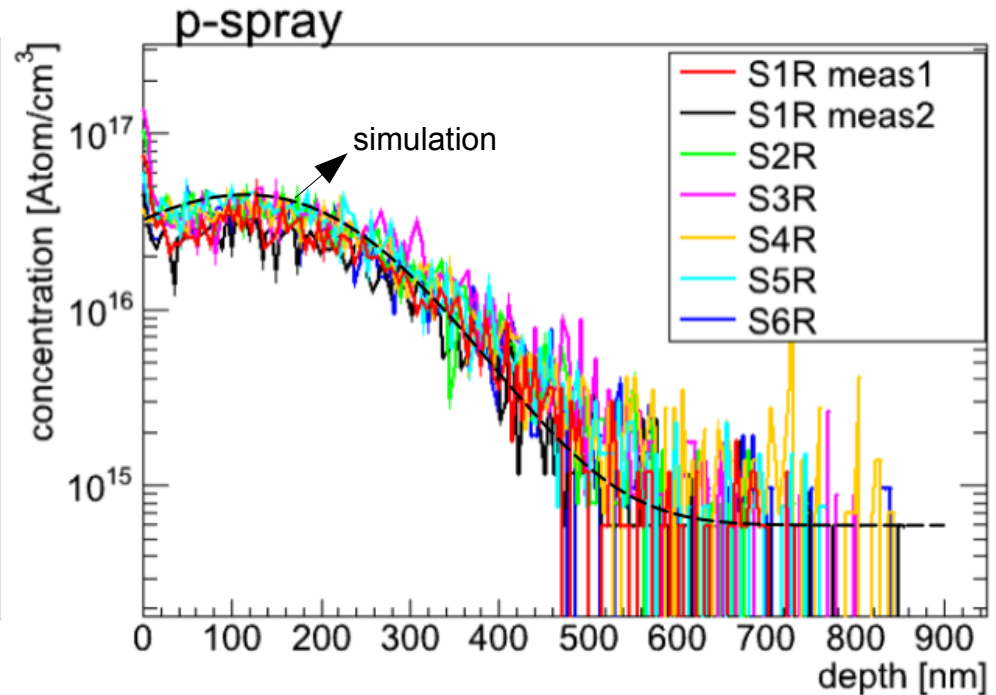
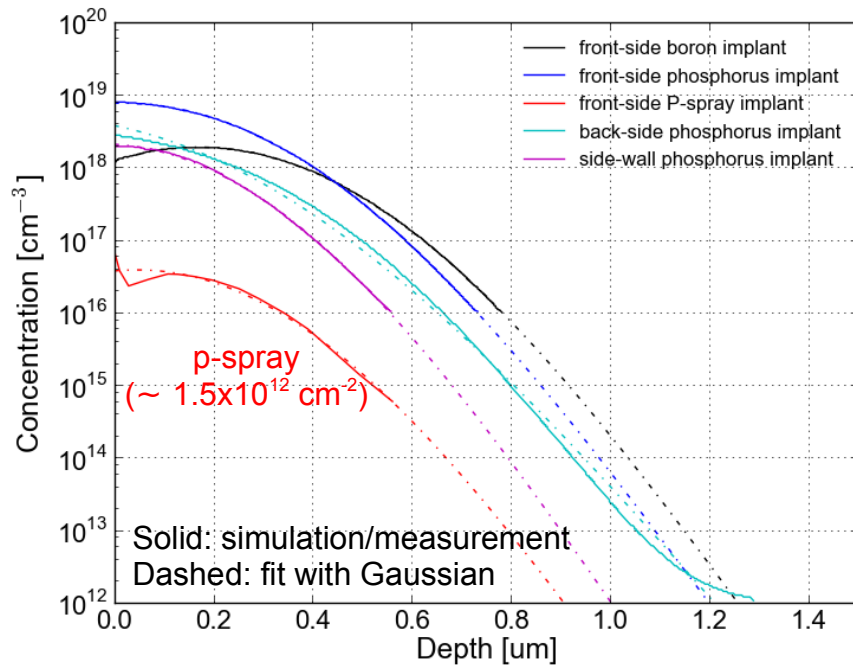
- Layouts and cross sections of edgeless sensors with active edges used in simulation
 - 6 different ones: p^+n , p^+p , n^+p and n^+n with p-spray, n^+p and n^+n with p-stop
 - Pixel pitch: $55\ \mu\text{m}$ (Medipix compatible)
 - Width of pixel implant: $30\ \mu\text{m}$; gap between pixel implants: $25\ \mu\text{m}$
 - Metal overhang: $5\ \mu\text{m}$
 - Last pixel-to-edge distance: $50\ \mu\text{m}$
 - Width of p-stop: $5\ \mu\text{m}$



Simulation of edgeless sensors: Input parameters

➤ Implant profiles (critical for breakdown simulation)

- All profiles obtained from the output of process simulation
- p-spray profile simulation result checked with SR measurement



➤ All profiles fit with Gaussian functions → fit parameters used as inputs in simulation

Simulation of edgeless sensors: Input parameters

➤ Parameters/physics models implemented in TCAD simulation

- Parameters extracted from measurements: MOS, diode, and GCD
- Radiation damage parameters used for breakdown simulation

Parameters:

	n-type silicon			p-type silicon	
	p ⁺ n	n ⁺ n (p-spray)	n ⁺ n (p-stop)	n ⁺ p (p-spray)	n ⁺ p (p-stop)
Doping	7 x 10 ¹¹ cm ⁻³			1.1 x 10 ¹² cm ⁻³	
T _{ox}	700 nm			680 nm	
e/h lifetime	equiv. 1.35 ms				
N _{ox}	1.0 x 10 ¹⁰ cm ⁻² (non-irra.) 3.0 x 10 ¹² cm ⁻² (irra.)			3.0 x 10 ¹⁰ cm ⁻² (non-irra.) 3.0 x 10 ¹² cm ⁻² (irra.)	
S ₀	1.35 cm/s (non-irra.) 12,000 cm/s (irra.)			3.54 cm/s (non-irra.) 12,000 cm/s (irra.)	
T _{si}	150 μm 300 μm 500 μm	150 μm 200 μm 300 μm 500 μm		150 μm 300 μm 500 μm	

Physics models:

- Drift diffusion
- Statistics: Fermi
- T = 293 K
- Band gap: band-gap narrowing
- Mobility: doping dependence, high-field saturation, carrier-carrier scattering and degradation at the interface
- Recombination: doping, temperature dependence and electric field enhancement
- Auger recombination
- Band-to-band tunneling with Hurkx model
- Avalanche: vanOverstraetenMan model with the gradient of quasi-Fermi potential as driving force
- Si-SiO₂ interface: surface recombination, fixed charge
- Boundary condition: Neumann

➤ Simulation done with fixed layout but different silicon thicknesses

➤ Only results on sensor active volume and breakdown for 300 μm thick sensor will be shown



Summary on sensor simulation

> Active volume/X-ray sensitive volume:

- Full active volume for n^+n and p^+p sensors
- Inactive volume at sensor corner of n^+p and p^+n sensors: sensor thickness, bias voltage, doping (and last pixel-to-edge distance) dependence

> Breakdown and radiation hardness:

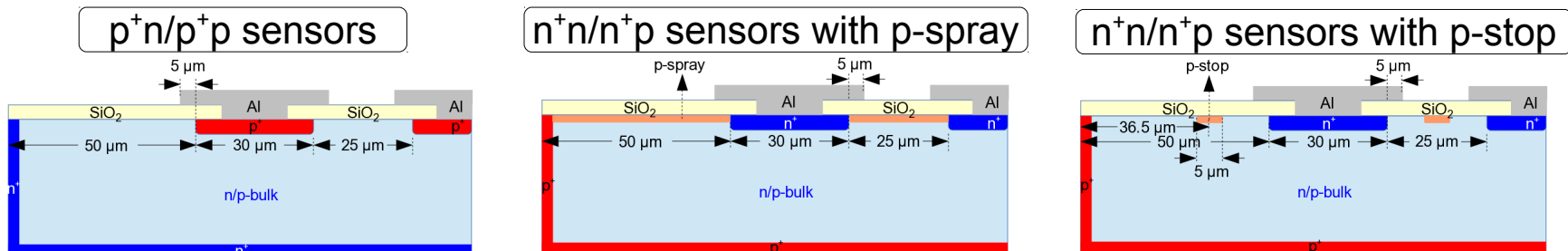
- High current due to breakdown flows into 1st pixel
- All sensor layouts/polarities stand for >180 V without irradiation
- Breakdown voltage gradually decreases with X-ray irradiation for p^+n , p^+p , and n^+n/n^+p sensors with p-stop
- n^+n/n^+p sensors with p-spray withstand certain irradiation with $N_{ox} \approx N_{p-spray}$
- Edge breakdown for n^+n/n^+p sensors with p-stop and with p-spray dose at high irradiation doses



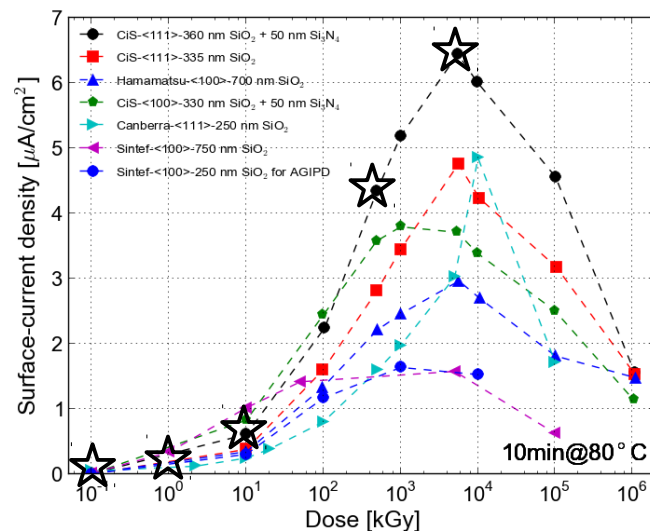
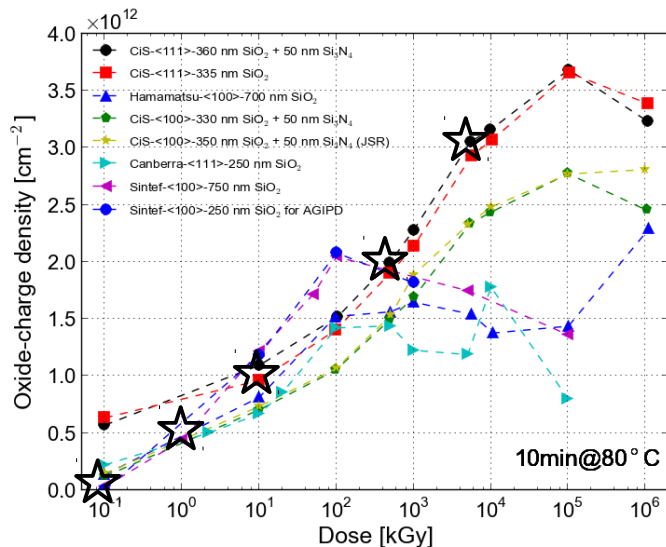
Simulation of commercial edgeless sensors

➤ Layouts and cross sections of commercial edgeless sensors

- 6 different ones: p^+n , p^+p , n^+p and n^+n with p-spray, n^+p and n^+n with p-stop
- Junction depth of $1.2\ \mu\text{m}$ and oxide thickness of $700\ \text{nm}$

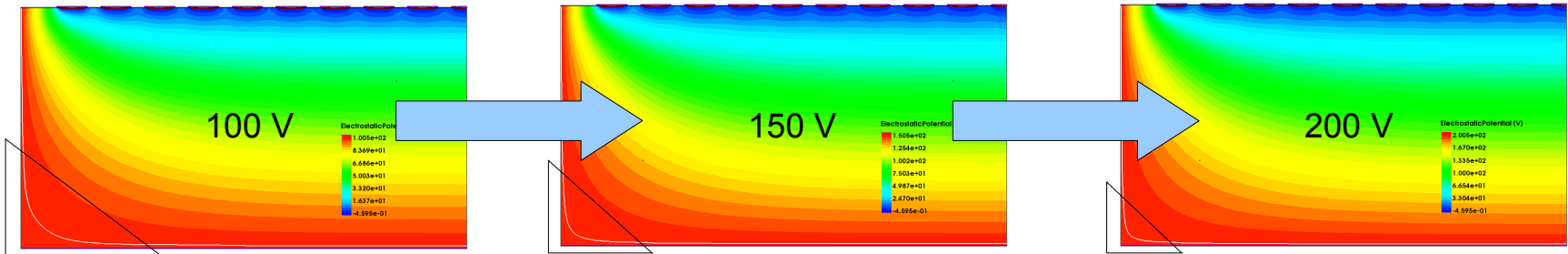


➤ Radiation-damage parameters (☆) from measurements implemented

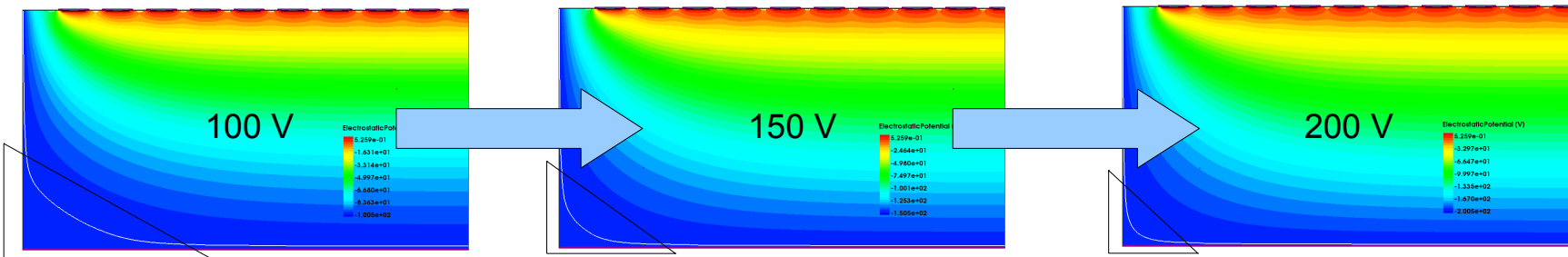


Simulation of sensor active/depletion volume

> Active (depletion) volume of p⁺n sensor



> Active volume of n⁺p sensor (with p-spray or p-stop)

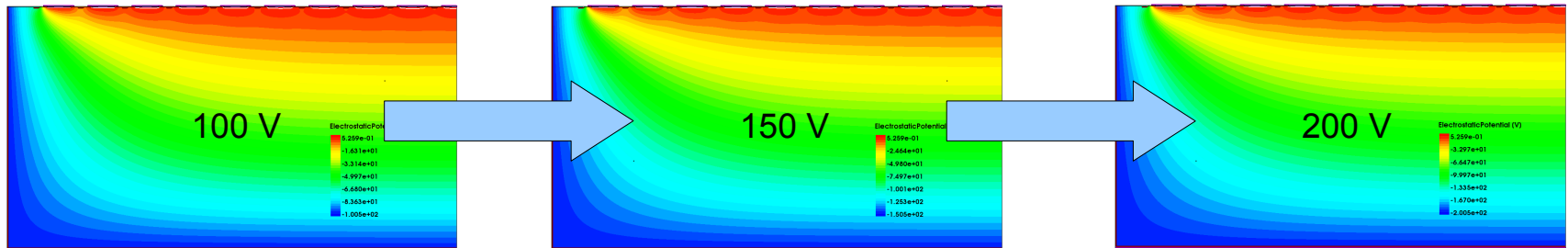


> Conclusion for p⁺n and n⁺p sensors:

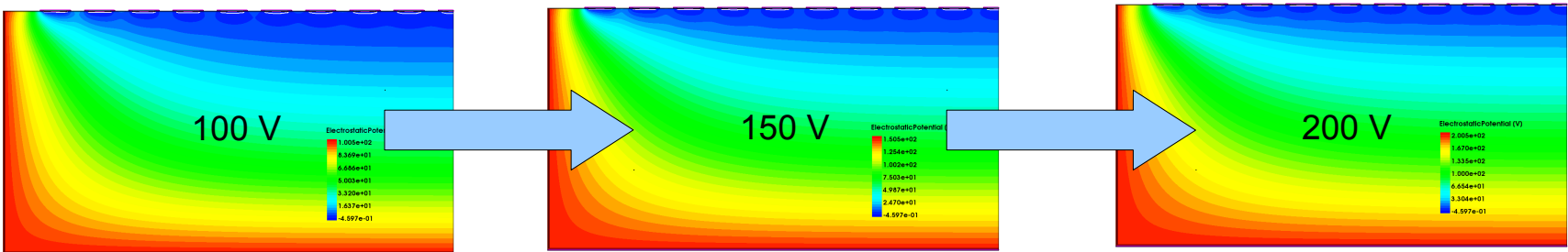
- Sensor depletion starting from pixels → inactive region at sensor corner
- Inactive volume shrinks with voltage (at least 100 V above V_{dep} needed?)
- Higher doping, thicker Si → larger additional voltage needed

Simulation of sensor active/depletion volume

> Active volume of n⁺n sensor (with p-spray or p-stop)



> Active volume of p⁺p sensor



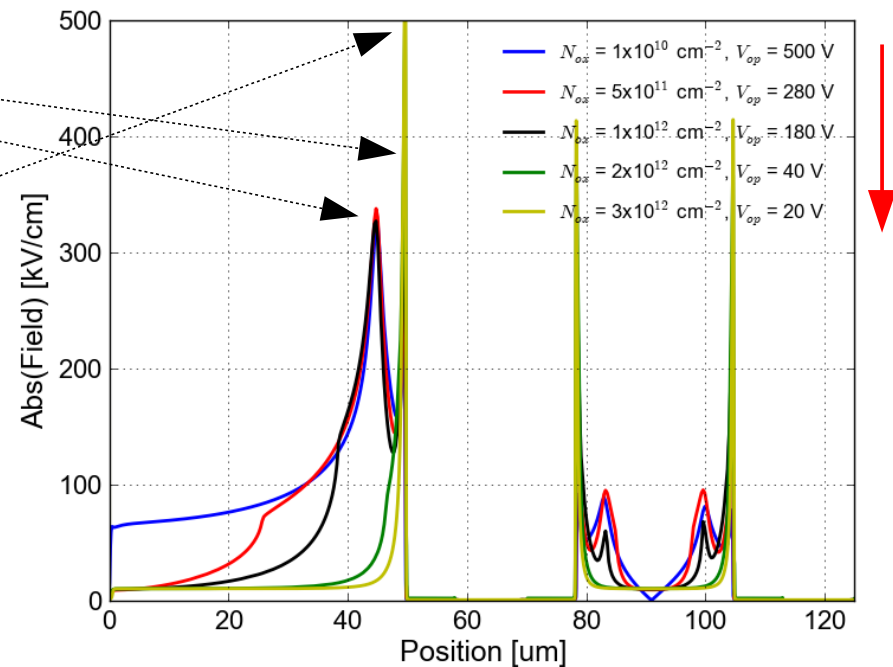
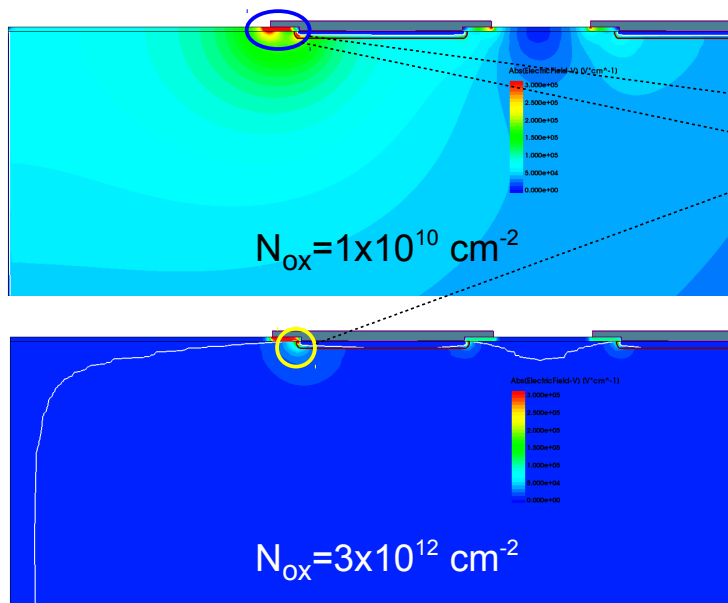
> Conclusion for n⁺n and p⁺p sensors:

- Sensor depletion starting from edge and backside → no inactive region
- No/Small additional voltage above V_{dep} needed (typically 10-15 V)

Breakdown simulation of p⁺n sensor

➤ High field region:

- $N_{ox} \leq 1 \times 10^{12} \text{ cm}^{-2}$, high field below metal overhang and at junction of 1st pixel
- $N_{ox} > 1 \times 10^{12} \text{ cm}^{-2}$, high field at implant junction of 1st pixel

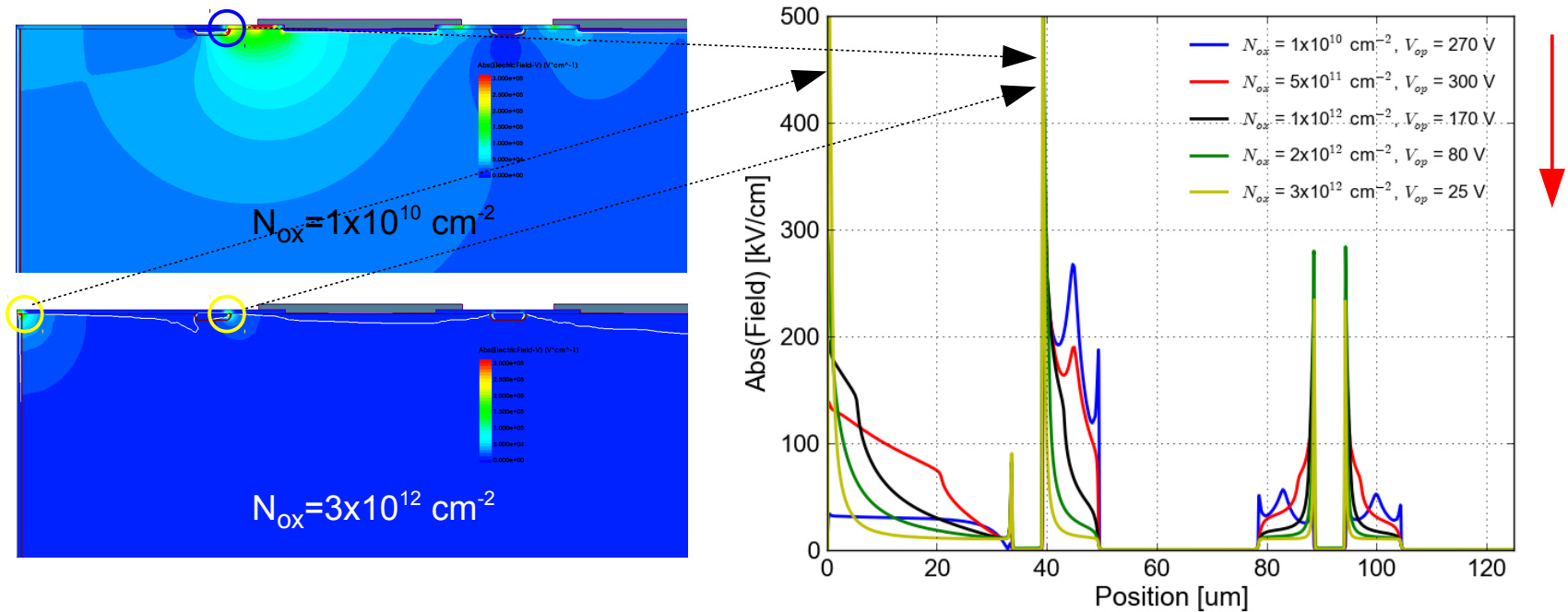


- 1st pixel behaves like CCR of a conventional sensor → breakdown first
- Breakdown voltage drops gradually with increasing oxide charges

Breakdown simulation of n⁺n/n⁺p sensors with p-stop

➤ High field region:

- $N_{ox} \leq 1 \times 10^{12} \text{ cm}^{-2}$, high field at implant junction of p-stop
- $N_{ox} > 1 \times 10^{12} \text{ cm}^{-2}$, high field at implant junctions of p-stop and sensor edge



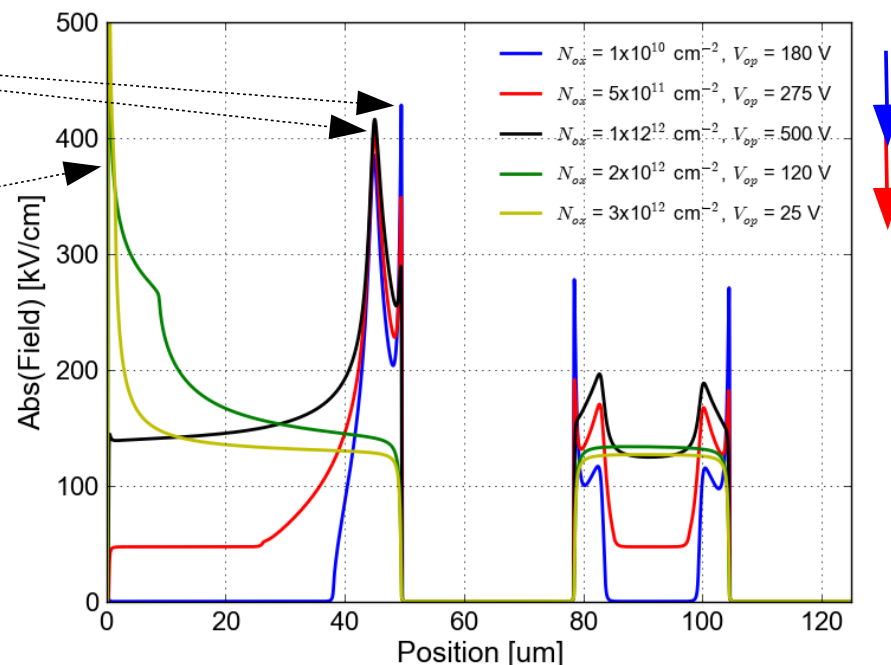
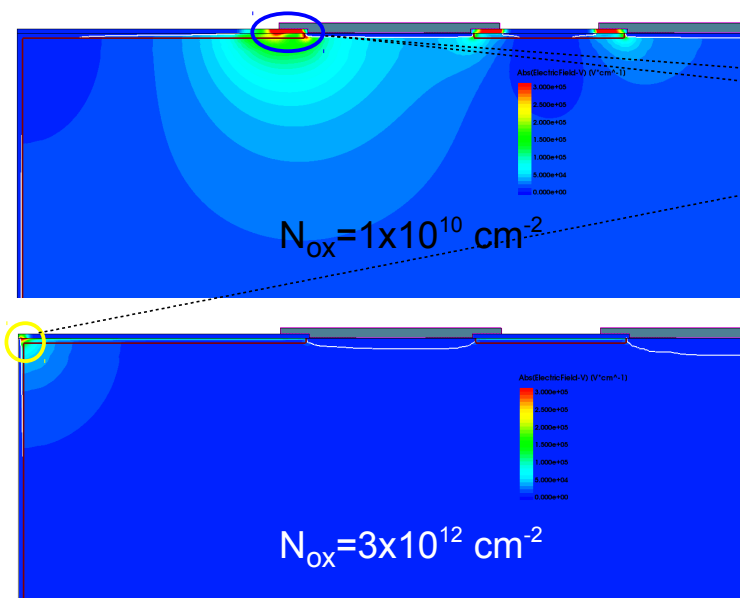
➤ High field at sensor edge ← direct exposure to oxide charges

➤ Breakdown voltage drops gradually with increasing oxide charges

Breakdown simulation of n⁺n/n⁺p sensors with p-spray

➤ High field region:

- $N_{ox} \leq 1 \times 10^{12} \text{ cm}^{-2}$, high field at pixel-implant/p-spray interface and below metal
- $N_{ox} > 1 \times 10^{12} \text{ cm}^{-2}$, high field at sensor edge

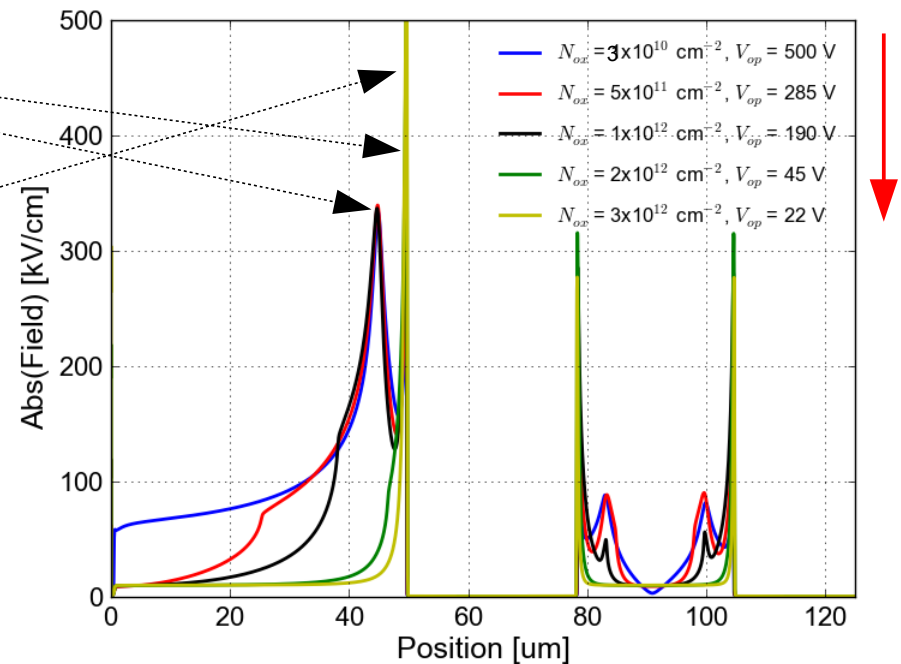
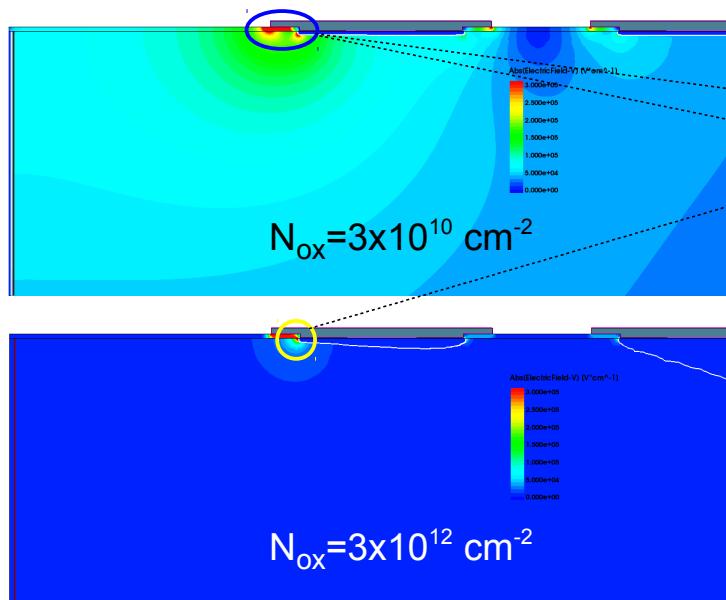


- High field at sensor edge → improved by increasing p-spray dose
- Breakdown improves with N_{ox} , but decreases when $N_{ox} > N_{p\text{-spray}}$

Breakdown simulation of p⁺p sensor

➤ High field region:

- $N_{ox} \leq 1 \times 10^{12} \text{ cm}^{-2}$, high field below metal overhang of 1st pixel
- $N_{ox} > 1 \times 10^{12} \text{ cm}^{-2}$, high field at implant junction of 1st pixel

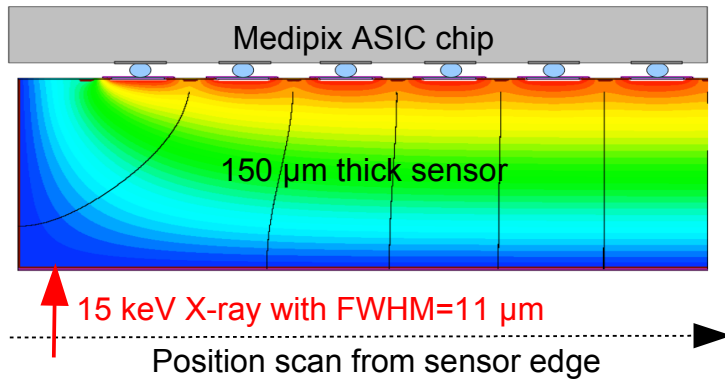


➤ Results (V_{bd} and high field region) similar to p⁺n sensor

➤ Breakdown voltage drops gradually with increasing oxide charges

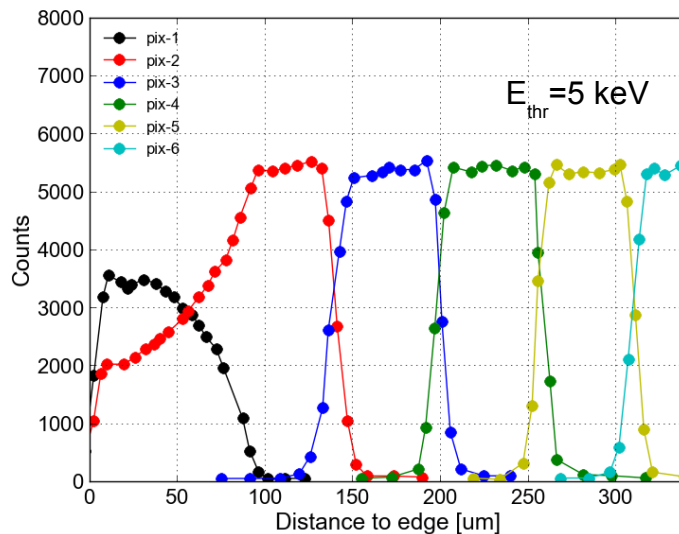
Charge-collection behavior: Measurement results on thin-Si

➤ X-ray scan on sensor backside (Uni-Glasgow@Diamond Light Source)

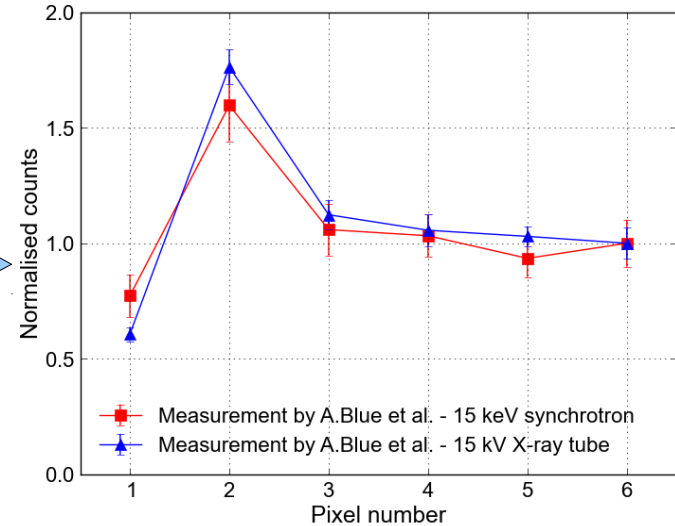


- Non-uniform charge collection
- Different counting behaviors in flat field image

Reason: bending electric field



integration

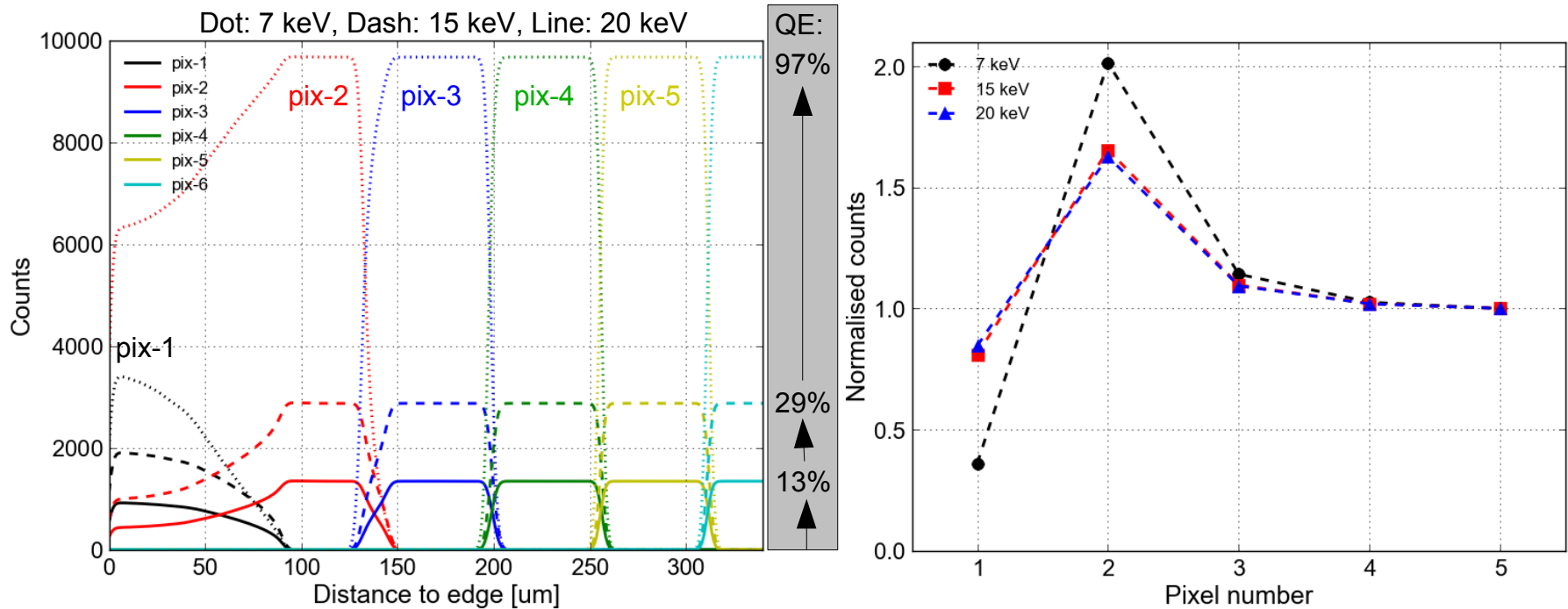
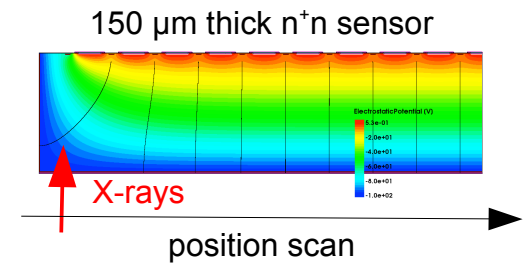


➤ Similar observation from mesh scan

Charge-collection behavior: Model calculation for 150 μm Si

➤ X-ray scan on sensor backside (10^4 entries):

- 7 keV, 15 keV and 20 keV X-rays (5 μm beam)
- 150 μm thick Si with 50 μm edge space
- Edge pixel counts vs. distance ($E_{\text{thr}} = E_{\text{x-ray}}/2$)

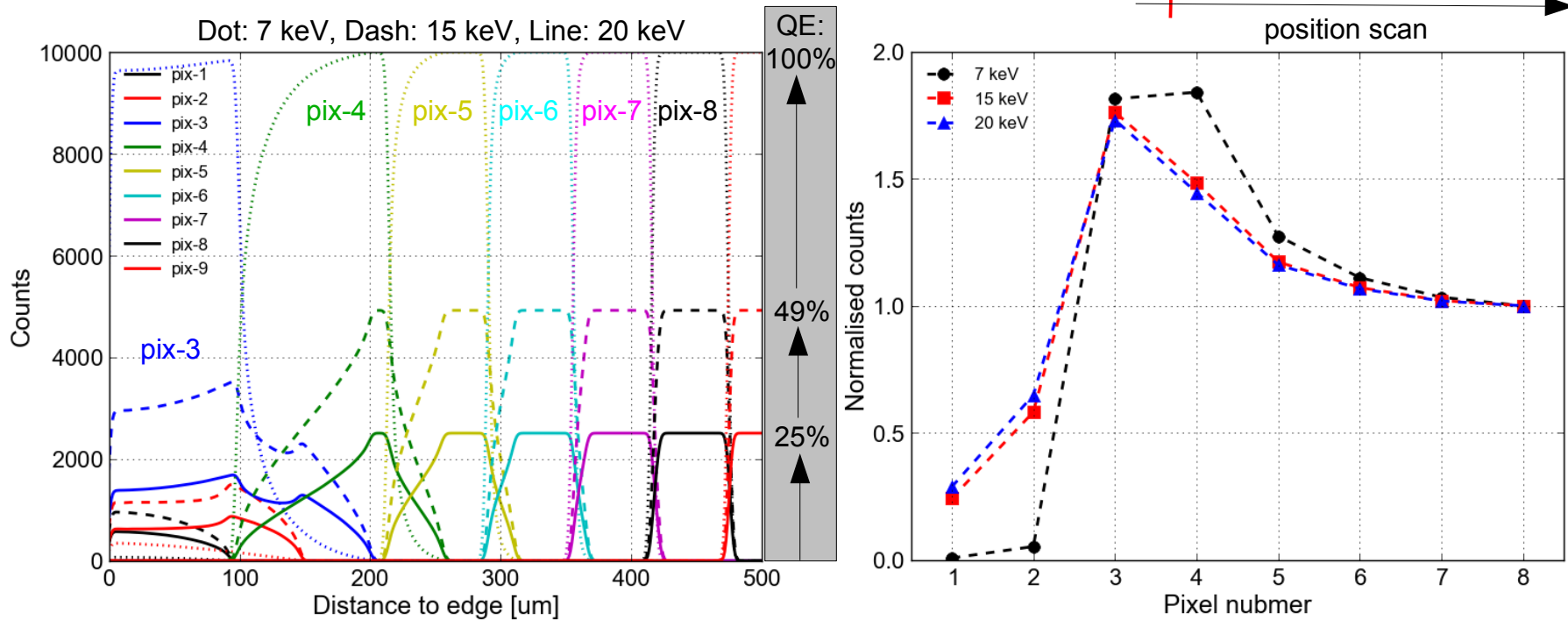
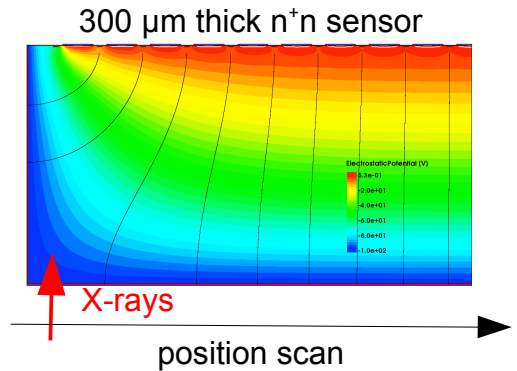


➤ Count of last edge pixel decreases with photon energy

Charge-collection behavior: Model calculation for 300 μm Si

➤ X-ray scan on sensor backside (10^4 entries):

- 7 keV, 15 keV and 20 keV X-rays (5 μm beam)
- 300 μm thick Si with 50 μm edge space
- Edge pixel counts vs. distance ($E_{\text{thr}} = E_{\text{x-ray}}/2$)



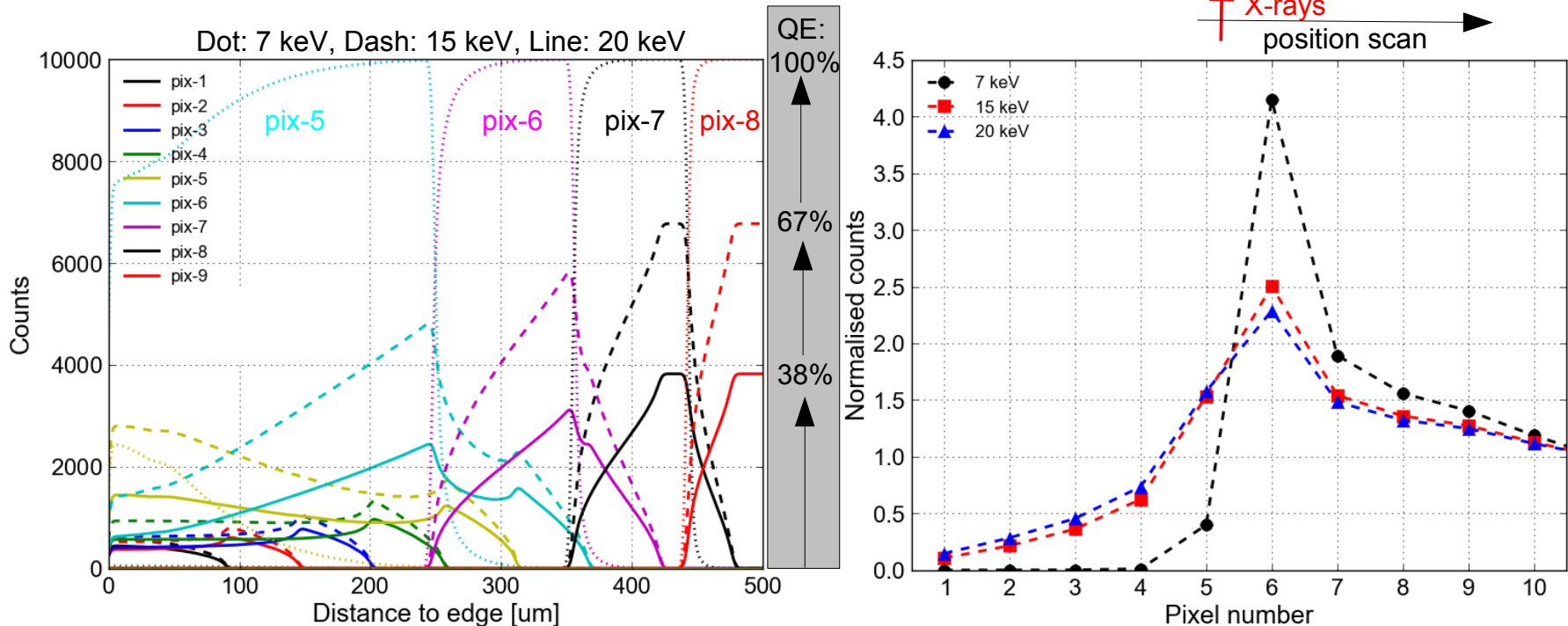
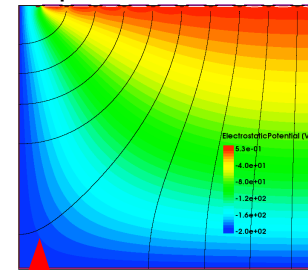
➤ Last two edge pixels respond to <10% 7 keV photons

Charge-collection behavior: Model calculation for 500 μm Si

➤ X-ray scan on sensor backside (10^4 entries):

- 7 keV, 15 keV and 20 keV X-rays (5 μm beam)
- 500 μm thick Si with 50 μm edge space
- Edge pixel counts vs. distance ($E_{\text{thr}} = E_{\text{x-ray}}/2$)

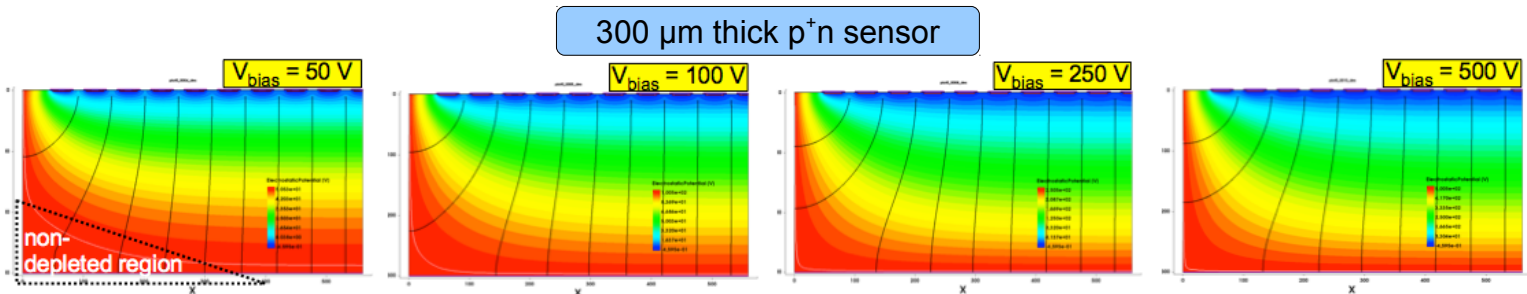
500 μm thick n^+n sensor



➤ Last four edge pixels respond to <10% 7 keV photons

Charge-collection behavior: Summary

- Non-uniform charge collection for edge pixels: X-ray energy, sensor thickness, last pixel-to-edge distance, and sensor polarity dependence
 - Low X-ray energy → good QE for central pixels but poor charge collection for edge pixels
 - Thin silicon and large last-to-edge distance → good charge collection for edge pixels but poor QE for high energy X-rays
 - Charge collection of p^+p sensor similar to n^+n sensor, p^+n similar to n^+p
 - Bending of electric field for p^+n and n^+p sensors are bias voltage dependent → voltage dependence of charge collection



- Conclusion: To obtain the optimized charge collection for edge pixels and guarantee the low energy photon sensitivity, last pixel-to-edge distance should be kept $> 50\%$ of the sensor thickness